

**END USER VOLTAGE REGULATION AT LOW-VOLTAGE  
DISTRIBUTION CONGESTION OF BATTERY CONNECTED  
MICRO-GRID**

**A thesis submitted**

**In partial fulfillment of the requirements**

**For the Degree of**

**MASTER OF TECHNOLOGY**

**In**

**POWER SYSTEM & CONTROL**

**(ELECTRICAL ENGINEERING)**

**By**

**Mr. VIVEK KUMAR SINGH**

**1170450006**

**Under the Guidance of**

**Prof. VikashPandey**

**Assistant Professor**

**BABU BANARASI DAS UNIVERSITY, LUCKNOW**

**To the**

**School of Engineering**



**BABU BANARASI DAS UNIVERSITY LUCKNOW**

**MAY 2019**

## **CANDIDATE'S DECLARATION**

I hereby declare that the work, which is being presented in the dissertation entitled “**END USER VOLTAGE REGULATION AT LOW-VOLTAGE DISTRIBUTION CONGESTION OF BATTERY CONNECTED MICRO-GRID**” in partial fulfillment for the award of degree of “**Master of Technology**” in Department of Electrical Engineering with Specialization in **Power System& Control** and submitted to the **Department of Electrical Engineering, Babu Banarasi Das University** is a record of my own investigations under the guidance of **Prof. Vikash Pandey, Assistant Professor Department of Electrical Engineering, Babu Banarasi Das University, Lucknow.**

I have not submitted the matter presented in this dissertation anywhere for the award of any other degree.

**(Vivek Kumar Singh)**

M..Tech Scholar (Power System& Control)

Roll No. : **1170450006**

Department of Electrical Engineering

School of Engineering

Babu Banarasi Das University, Lucknow.

## **CERTIFICATE**

This is to certify that the work contained in this thesis, titled “**END USER VOLTAGE REGULATION AT LOW-VOLTAGE DISTRIBUTION CONGESTION OF BATTERY CONNECTED MICRO-GRID**” has been successfully carried out by the **Vivek Kumar Singh**(Roll No. :**1170450006**), from Babu Banarasi Das University, Lucknow has been carried out under my/our supervision and this work has not been submitted elsewhere for a degree.

**Signature**

**VIKASH PANDEY**

**Assistant Professor**

Department of Electrical Engineering

School of Engineering

BabuBanarasi Das University, Lucknow.

May 2018-19

**Place:**

**Date:**

## ABSTRACT

In this dissertation, a new approach is projected for analysis on End user voltage regulation at low voltage distribution congestion of battery connected micro grid. Projected technique is based on the power control and voltage regulation.

The working principle of described method is that the grid is developed by the solar system for the distribution of energy and control on congestion.

In this thesis, the study of the photovoltaic system with maximum power point controller has been developed. From the theory of the photovoltaic, a mathematic model of the PV has been presented. Then, the photovoltaic system with DC-DC boost converter; maximum power point controller and resistive load have been designed. Finally, the system has been simulated with Simulink /MATLAB.

First, the simulations of the PV panels showed that the simulated models were accurate to determine the characteristics voltage current because the current voltage characteristics are the same as the characteristics given from the data sheet. In addition, when the irradiance or temperature varies, the PV models output voltage current change. Then, the simulation showed that Perturb and observe algorithm can track the maximum power point of the PV, it always runs at maximum power no matter what the operation condition is. The results showed that the Perturb and observe algorithm delivered an efficiency close to 100% in steady state.

The simulations of the PV with maximum power point, boost converter and resistive load were performed by varying the load, the irradiance.

Finally, the PV performance and the maximum power point was analyzed, and the three phase full bridge DC-AC inverter was simulated with grid. The results showed that the DC voltage generated by the PV array could produce an AC current sinusoidal at the output of the inverter. The amplitude of the current depends on the PV power.

## ACKNOWLEDGEMENT

It gives me immense pleasure to express my sincere gratitude toward my supervisor **Prof. Vikash Pandey**, Assistant Prof. Electrical Engineering, SoE Babu Banarasi Das University, Lucknow for his scholarly guidance. It would have never been possible for me to take this dissertation to completion without his innovative ideas and his relentless support and encouragement. I consider myself extremely fortunate to have had a chance to work under his supervision. In spite of his hectic schedule he was always approachable and spared his time to attend my problems. I am also thankful to **Mr. Shashikant**, Electrical Engineering, SoE Babu Banarasi Das University, Lucknow.

I would like to express my special thanks to **Prof. V.K. Maurya**, Associate Professor & Head Department of Electrical Engineering, School of Engineering Babu Banarasi Das University, Lucknow for their kind support.

I also express my gratitude to all the respected faculty member of Electrical Engineering, SoE Babu Banarasi Das University, Lucknow for their kind support who have helped me directly or indirectly in completion of this dissertation.

I am really thankful to *Department of Electrical Engineering*, School of Engineering, Babu Banarasi Das University, Lucknow for all the technical facilities both infrastructural and rich faculty due to which my dream of achieving M.Tech. could prove true.

Finally, yet importantly, I would like to express my heartfelt thanks to my **Parents** to give invaluable support in all the circumstances that exhibited a high degree of patience and kept my moral always high.

**Vivek Kumar Singh**

# CONTENTS

<b>TITLE</b>	<b>PAGE NO.</b>
CANDIDATE'S DECLARATION	ii
CERTIFICATE	iii
ABSTRACT	iv
ACKNOWLEDGEMENT	v
CONTENTS	vi
LIST OF FIGURES	x
LIST OF TABLES	xiv
LIST OF ABBREVIATIONS	xv
LIST OF SYMBOLS	xvi
ABSTRACT	1
1. Introduction	2
1.1 Project Background	2
1.2 Photovoltaic Market	3
1.3 Typical application of the PV system	3
1.4 Photovoltaic system and energy storage	4
1.5 Thesis Outline	4
2. Literature Survey	6
2.1 Potential Energy of Photovoltaic System	6
2.2 Different technology of Photovoltaic's	7
2.3 Electrical Equivalent of Solar Cells	11
2.3.1 The other benefits	17
2.3.2 Tie-line Control Design	17
2.4 Grid Connected PV System	18
2.5 Solar Cell and its Characteristics	19
2.6 Converters and Inverter	25
3. System Description and Modeling of the Photovoltaic System	30
3.1 General topology of photovoltaic system	30
3.2 Photovoltaic array modeling	32
3.2.1 Curves I-V Characteristics of the PV array	32

3.2.2 Model of the PV cell	33
3.2.3 Model of the Photovoltaic module	35
3.2.4 Photovoltaic array	36
3.3 DC/DC converter	38
3.3.1 Operation of the boost converter	38
3.3.2 Selection of the inductor	41
3.3.3 Power decoupling capacitor	41
3.4 Six step inverter	41
3.5 Modulation strategies	44
3.5.1 SVPWM techniques	44
3.5.2 Sine PWM	49
3.6 Control of the boost converter with MPPT controller	51
3.6.1 Maximum power point techniques for PV	51
3.6.2 Perturb & Observe P&O/ Hill Climbing	52
4. Simulation of the Photovoltaic System Using MATLAB / Simulink	54
4.1 Simulation of the photovoltaic module	54
4.2 Simulink model of boost converter	56
4.3 Simulink model of the photovoltaic system with AC-DC-AC PWM Converter	57
4.4 Simulink model of the photovoltaic system with MPP	57
4.5 Simulink model of the photovoltaic system with MPPT and Battery	58
4.6 Simulink model of Grid connected Photovoltaic system	59
5. Simulation Result of the Photovoltaic System Using MATLAB / Simulink	61
5.1 Simulation result of photovoltaic system	61
5.2 Photovoltaic array characteristics	61
5.2.1 The I-V and P-V characteristics of single cell	61
5.3 Photovoltaic system with a Boost converter	63
5.3.1 R-L type load	64
5.3.2 Change input voltage waveform of DC-DC converter with 400 V Constant	65
5.3.3 DC-DC converter	65
5.3.4 Photovoltaic connected to a three-phase inverter	66

5.4 PV system connected with load including MPPT and Battery	69
5.4.1 PV system connected with load including MPPT	68
5.4.2 PV system connected with load including MPPT and battery	69
5.5 Grid connected PV system	70
6.Conclusion	78
6.1 Conclusion	78
6.2 Future Research	78
References	79
Appendix	81
Plagiarism Report	82
LIST OF PUBLICATION	83
CERTIFICATE OF FINAL THESIS SUBMISSION	84
CV	85



## LIST OF FIGURES

FIGURE NO.	DESCRIPTION OF FIGURE	PAGE NO.
Chapter - 2		
2.1	Resources Energy Trend	7
2.2 (a)&(b)	Single jn. Amorphous&Cells connected in series	8
2.3	Multiple-jn. Stacked or tandem solar cells where two or more Current-matched cells are stacked on top of one another	8
2.4 (a)& (b)	Mixed-phase microcrystalline/amorphous material & Single-phase Polycrystalline film.	9
2.5	Crystalline silicon on glass (CSG) unit cell structure	9
2.6	Device schematic for a cadmium telluride cell	10
2.7	Basic CIS (copper indium diselenide) cell structure	10
2.8	Summary on how solar cells work	12
2.9	Model for single solar cell	12
2.10	A typical current-voltage ( <i>I-V</i> ) curve for a solar cell	13
2.11	The PV from cell to module	14
2.12	PV module consists of parallel and series cells	14
2.13	Solar cells array consist of $M_p$ parallel branches each with $M_s$ Modules in series	15
2.14 (a)& (b)	Series-parallel configuration for PV generator&M-VAR Block Diagram	15
2.15	Grid-connected PV System	18
2.16	A detailed Grid-Connected PV System	19
2.17	Characteristic <i>I-V</i> curve of a practical photovoltaic device	20
2.18	Characteristic <i>I-V</i> curve of the photovoltaic cell	20
2.19(a) & (b)	Characteristic shown on the influence of ambient irradiation &Characteristic shown on the influence of cell temperature	21
2.20 (a)& (b)	The <i>I-V</i> curve responses with two identical cells connected in Series.&The <i>I-V</i> curve responses with two identical cells connected in parallel	22
2.21	Electrical characteristics of Sharp NE-80EJEA solar cell	23
2.22	Electrical characteristics of Sharp NE-80EJEA solar cell	23

2.23	The Schematic of a Buck Converter	25
2.24	Connection of Inverter	27
2.25	Full Bridge Voltage Source Inverter	28
Chapter - 3		
3.1	First stage in modeling the solar cell	30
3.2	Structure of Single stage DC/AC Photovoltaic system	31
3.3	Structure of dual stage DC/DC and DC/AC Photovoltaic system	31
3.4	Topology of PV with boost converter and resistive load	31
3.5	Topology dual stage three-phase photovoltaic system with resistive Load	32
3.6	I-V Characteristics of the PV as function of irradiance	32
3.7	I-V Characteristics of the PV as function of Temperature	32
3.8	I-V curve, P-V curve with the MPP	33
3.9	Equivalent circuit of solar cell with one diode	33
3.10	Circuit model of the photovoltaic module	36
3.11	PV Array composed of $N_{ser} \times N_{par}$ modules	36
3.12	Model structure of the photovoltaic array	37
3.13	Topology of Boost converter	38
3.14	Schematic diagram of Boost converter	39
3.15	Diagram when switch $T_1$ is on and $D_1$ is off	39
3.16	Diagram when switch $T_1$ is off and $D_1$ is on	39
3.17	Output waveform of DC/DC converter	40
3.18	Harmonic of output voltage when $\alpha$ is 10	42
3.19	Three-phase six-step inverter	42
3.20	Waveforms of the switching functions	43
3.21	Phase voltage normalized spectrum	44
3.22	Eight switching states	45
3.23	Switching vectors and the 6 sectors	45
3.24	Space vector PWM switching patterns and sector duration	48
3.25	Sine triangle, voltage reference and phase voltage	49
3.26	Block diagrams of MPPT with P&O	52
3.27	Block diagrams of MPPT with Hill Climbing	52

3.28	Principle of P&O	52
Chapter - 4		
4.1	Simulation of the PV module	54
4.2	Simulation of the PV array	55
4.3	Grid connected system	55
4.4	Simulation of the DC-DC converter	56
4.5	Simulink model of the photovoltaic system with dc-dc converter	56
4.6	Simulation of the PV system with boost and three-phase inverter	57
4.7	Simulation of the PV system with MPPT	57
4.8	Simulation of the dc to dc converter with MPPT	58
4.9	Simulation of the perturb and observe algorithm	58
4.10	Simulation of the PV system with MPPT and battery	58
4.11	Interconnection between grid and inverter	59
4.12	Grid synchronizing	59
4.13	Simulation of Grid connected Photovoltaic system	59
Chapter - 5		
5.1	I-V curve and P-V curve of the BP MSX 120 module	61
5.2	I-V curve and P-V curve of the BP MSX 120 module	62
5.3	I-V curve and P-V curve of the BP MSX 120 module	62
5.4	(a) DC I/P Voltage (b) DC I/P Current	64
5.5	(a) DC Bus Voltage(b) DC Bus Current	64
5.6	(a) Input Voltage (b) Input Current	65
5.7	(a) DC Bus Voltage (b) DC Bus Current	65
5.8	(a) Input Volts (b) Input Current	65
5.9	(a) DC Bus Voltage (b) DC Bus Current	65
5.10	Sinusoidal load voltage (Vab&Vdc)	66
5.11	(a)Vab Inverter (b)Vab load	66
5.12	Battery connected to a three-phase inverter(Modulation index)	66
5.13	VdcVab Inverter	67
5.14	Vab Load Modulation Index	67
5.15	Insolation at 1000 W/m <sup>2</sup> Vdc&Vab Inverter	70
5.16	Vab Load&Modulation Index	70

5.17	Battery Voltage & State Of Charge	70
5.18	Vdc	71
5.19	Waveform of DC bus I dc	72
5.20	Waveform of active and reactive power	72
5.21	Waveform of terminal voltage	73
5.22	Waveform of $V_{abc}$ and $I_{abc}$	74
5.23	Waveform of DC bus Vdc & Idc	74
5.24	Waveform of active and reactive power	74
5.25	Waveform of terminal voltage	75
5.26	Waveform of $V_{abc}$ and $I_{abc}$	75
5.27	Waveform of DC bus	76
5.28	Waveform of active and reactive power	76
5.29	Waveform of terminal voltage Vabc (I/B)	76
5.30	Waveform of $V_{abc}$ and $I_{abc}$	77

## TABLES

TABLE NO.	DESCRIPTION OF TABLE	PAGE NO.
Chapter - 2		
2.1	Summarize The Different Technology In Thin Film Technology	7
2.2	Confirmed Terrestrial Module Efficiencies Measured Under The Global Am 1.5 Spectrum	11
2.3	Comparison Between Different Connections Topologies Of Pv Systems	15
2.4	Pv Module Characteristic For Standard Technologies	24
2.5	The Switches State For A Full Bridge Single Phase Inverters	28
Chapter-3		
3.1	Pv Module Bp Msx120 Datasheet At Stc	35
3.2	Switching States Of The Inverter Switches	46
Chapter – 5		
5.1	Photovoltaic Module Maximum Power Point Values At 1000, 800 & 600w/M <sup>2</sup>	62
5.2	Pv Module Ne-80ejea Data Sheet Values At Stc	63
5.3	Characteristics Of 26 Kw Photovoltaic	63
5.4	$R = 100 \times 100 / 6000 = 1.666 \Omega$ , $L = 100 \times 100 / 6000 = 1.666 \text{ H}$	64
5.5	Input /Output	65
5.6	Parameters Of 26 Kw Photovoltaic Systems	67
5.7	Reading Of V, I, P, & D	68
5.8	Reading Of P & I <sub>battery</sub> (50 Kw Load) Reading Of Grid Connected System At Different Insolation	69
5.9	Reading Of Grid Connected System At Different Insolation	71

## LIST OF ABBREVIATIONS

### ABBREVIATIONS

### DESCRIPTION

NOCT	Nominal Operating Cell Temperature
PVS	Photovoltaic System
DC	Direct current
AC	Alternating current
CCM	Continuous Conduction Mode
DCM	Discontinuous Conduction Mode
MPP	Maximum power point
PWM	Pulse width modulation
MA	Modulation index
RMS	Root mean square
D	Diode
PF	Power factor
PVA	Photovoltaic array

## LIST OF SYMBOLS

SYMBOL	DISCRIPTION
$T_a$ (°C)	Ambient temperature
$\eta$	Efficiency
$\eta_r$	PV module efficiency at reference temperature ( $T_r = 25$ °C)
$\beta_p$	Temperature coefficient for module efficiency (% / °C)
$T_r$	Reference Temperature (25 °C)
$\eta_p$	Array average efficiency
$A$	Area of the array
$\bar{H}_t$	Solar radiation
$E_p$	Energy delivered by the PV array
$\lambda_p$	Miscellaneous PV array losses
$\lambda_c$	Other power conditioning losses
$E_p$	Energy delivered by the PV array
$E_A$	Energy available to the load
$\eta_{inv}$	Inverter efficiency
$E_{dlvd}$	Energy delivered to load
$\eta_{abs}$	PV energy absorption rate
$E_{grid}$	Energy available to the load
$I_R$	Load current
$I_{PH}$	Light-generated current or photocurrent
$I_S$	Cell saturation of dark current
$k$	( $1.38 \times 10^{-23}$ J/K) is a Boltzmann's constant
$T_C$	Cell's working temperature

$R_{SH}$	Shunt resistance
$R_S$	Series resistance
$J_{cell}$	Current density
$V_{cell}$	Voltage
$J_{ph}$	Induced photocurrent density
$J_{d1}$	Dark current density due to the carriers diffusion
$J_{d2}$	Dark current density due to the carriers recombination
$E_g$	Band gap energy
$Q$	$1.6 \times 10^{-19}C$ is an electron charge
$I_{ph}$	Currents generated by the solar cells (A)
$R_s$	Resistance series ( $\Omega$ )
$R_p$	Resistance parallel ( $\Omega$ )
$G_a$	Irradiance from the sunlight ( $W/m^2$ )
$T$	Cell temperature (K)
$I$	Output current of the PV (A)
$V$	Output voltage of the PV (V)
$V_{oc}$	Open circuit voltage (V)
$I_{sc}$	Short-circuit current (A)
$P_{mp}$	Power at maximum power point
$V_{mp}$	Voltage at maximum power point
$I_{mp}$	Current at maximum power point
$I_{ph}$	Photon produced by the cell
$I_d$	Diode current
$I_0$	Reverse saturation current of diode



$V_d$	Diode voltage
$D_m$	Duty cycle of the switch at maximum converter input power
$f_s$	Switching frequency
$V_{om}$	Maximum of the dc component of the output voltage
$\Delta I_{Lripple}$	Ripple current of the inductor
$I_{om}$	Output current at maximum output power
$V_{pv\_nmpp}$	PV output voltage at maximum power point
$V_{load}$	Output voltage of the boost converter
$\Delta V_{load}$	Output ripple voltage
$V_{tria}$	Peak amplitude of the triangular carrier
$V_{ref: peak}$	Amplitude of the sinusoidal reference signal
$N_s$	Number of cells in series
$N_{pp}$	Number modules in parallel
$N_{ss}$	Number of modules in series
$I_{scn}$	Nominal short-circuit voltage
$K_p$	Voltage temperature constant
$K_i$	Current temperature coefficient

# CHAPTER 1

## INTRODUCTION

### 1.1 Project Background

Photovoltaic System (PV) is getting popular by day as the crude oil price increases and unstable in the global market. Furthermore with green peace movement, and the consciousness of mankind has heightened up regarding green energy, photovoltaic may be one of the solution for better as well cleaner energy as it is naturally harness from the Sun energy. Although the technology is mainly well known in the space mission, yet it's still an alien for domestic usages. This is due to the high initial cost, generation efficiency and reliability. On the other hand, to answer the cry for alternative energy has made the PV system again popular among the researchers. Having said so, the rural areas where the grid connection is extremely expensive, PV Systems have been implied to give hope to these areas, while for the urban life, the PV Water Heater is common and can be found on the roof of the houses.

Currently, more than 3500MW of photovoltaic system have been installed all over the world. Referring to the results from Earth Policy Institute (EPI), the world production of solar PV cells increased 32% in 2003, compared to the most recent 5-year average of 27% a year. Production increased to 742 MW, with cumulative global production at 3145 MW at the end of year 2003, enough to meet the electricity niche of one million homes. Referring to the EPI, this extraordinary growth is driven to some degree by improvements in materials and technology, but primarily by market introduction programs and government incentives. This fact can clearly conclude that this solar energy (photovoltaic) is a very promising as next generation energy source.

In this context, lots of research needs to be done in order to achieve a reliable and efficient energy. Looking at the grid connected system, where by the system mainly consists of photovoltaic (PV) modules, inverter, battery, and switching point for the utility. Different types of photovoltaic cell will yield different energy output; meanwhile the controlling technique of inverter is very crucial in championing the PV system. Inverter design should

consider the size and capacity of the plant, on the other hand choosing the right controlling technique is needed as well in order to achieve an efficient renewable energy system.

There are many types of inverter used in converting the direct current (DC) produced by the PV to alternating current (AC). The conversion is a must in order to suit the AC grid system that have been implemented and practiced for so long. Some of the types that can be used are multilevel inverters such as fly back capacitor, neutral point clamped multilevel inverter, diode clamped inverter and many more. Each topology has its own plus point and drawbacks depending on the usage of it. Applying certain controlling techniques to the inverters' such as Pulse Width Modulation (PWM), Space Vector Pulse Width Modulation (SVPWM), Step Modulation etc, the efficiency of the conversion can be obtained up to an optimum level. Hence this is another part for research in the PV Grid-Connected system.

On the other hand, there are many types of technology used in producing the photovoltaic cell, such as using the Silicon Photovoltaic (crystalline silicon, nano crystalline), Thin Film solar cells amorphous silicon, cadmium telluride, gallium arsenide, copper indium gallium and Concentrating Photovoltaic (multi junction cells). As said above, the different types and topologies of photovoltaic gives different energy output, such as the amorphous silicon typically efficiency is 6%-8%, while multi crystalline is 11% - 14%, and mono-crystalline is 12% - 17%, etc. Hence in this work, the major part of research will be a study on the impact of the different topologies of PV cells on the energy output generated.

Besides that, it's a common knowledge that, the PV system has different seasonal pattern behavior depending on the temperature as well as the solar irradiation. Due to the different temperature co-efficient of voltage and current the PV system has different output. Yet, to simplify the work of manufacturer mostly, the PV modules are rated at STC (standard test conditions) of solar irradiation as  $1000 \text{ Wm}^{-2}$ , while the spectrum is fixed and related to a sun-spectrum at air mass of 1.5 ( $AM = 1.5$ ).

As a conclusion, it's worthwhile to research on this photovoltaic system as it is the next generation energy source, while it's green and promotes to cleaner world. On top of that, this research work is in line with the government aspiration on becoming a greener nation with a renewable energy sources.

## **1.2 Photovoltaic Market**

Photovoltaic (PV) installation's capacity was completed during 2010 and has increased by over 55 per cent in comparison to 2009, along with that the typical size of the PV system is also expanding. Significant incentives program are being offered by many states and as a result, the PV market is expanding to those different states. Long-term situation of the solar market looks bright. A steady decline of the solar PV costs is expected, A Photovoltaic Array Simulation Model for MATLAB-Simulink GUI Environment [1]. Presumably as much as 50% within the next 4 to 7 years. The primary aim is to reduce the expenses related to the installation and the PV panel. In 2015, the target is to decrease the price for residential use to 8- 10 cents kWh. At this price, the solar PV will be affordable for the masses.

Several ways were attempted in order to bring down the expenses of the PV. Bringing down the costs of manufacturing, augmenting performance along with expanding upon the reliability of the technologies that are being used was few. Another important avenue where costs could be brought down was the local interaction and learning by means of an expanded capacity of manufacturing. A forecast suggests that electricity will be stable and consistent through 2025; elements such as tax legislation for carbon, fuel prices on a global level, facility/importation constructions, and costs of labor, inflation and exchange rates could act as contributor to the achievement parity of solar energy with electricity prices even faster than presently projected.

The solar market cost goal will be achieved with "5-10GW of PV fitted by 2015 within the country and over 70-100 GW by the year 2030."

## **1.3 Typical application of the PV system**

Photovoltaic systems have become an energy generator for a wide range of applications. The applications could be standalone PV systems or grid connected PV systems. A standalone PV system is used in isolated applications where PV is connected directly to the load and storage system. With a standalone photovoltaic, when the PV source of energy is very large, having energy storage is beneficial. Whereas a PV system that is connected through a grid is used

when a PV system injects the current directly into the grid itself. The advantage of the grid-connected system is the ability to sell excess of energy.

#### **1.4 Photovoltaic system and energy storage**

The main benefit of integrating storage with renewable energy is the capability of shifting the peak demands using charging/discharging (charging when the excess electricity is stored, discharging when there is a peak demand). The storage can be charged from the renewable sources or from the grid. The demand on the grid can be met with the renewable sources (wind, solar) or energy storage or both.

The other benefits are:

**“Mitigation of short-term solar power intermittency and wind gust effects and minimizing its impacts on voltage, frequency, and power fluctuations in power system”**

**“Lowering the transmission and distribution costs by increasing the confidence in renewable distributed generation”**

- Improving power system stability
- Reduction of harmonics

The use of renewable energy increased greatly just after the first big oil crisis in the late seventies. At that time, economic issues were the most important factors, hence interest in such processes decreased when oil prices fell. The current resurgence of interest in the use of renewable energy is driven by the need to reduce the high environmental impact of fossil-based energy systems. Harvesting energy on a large scale is undoubtedly one of the main challenges of our time. Future energy sustainability depends heavily on how the renewable energy problem is addressed in the next few decades.

#### **1.5 Thesis Outline**

This theses will is a compilation of many chapters that will elaborate in stages the research work that have been carried out. As in general this thesis mainly consist of five main chapters; introduction, literature review, circuitry buildings and simulation using MATLAB / SIMULINK software, simulation results analysis and conclusion.

In **chapter 1**, this thesis will discuss the research project in collectively. This chapter explained the crucial aspect of the research work such as background studies, objectives, research scopes and methodology as well the thesis outline will also be discussed finally.

**Chapter 2** completely dedicated to literature review about the grid connected PV system. This chapter will be solely theoretical in detail discussing on the types photovoltaic cell, inverters, and the whole system about it. In this academic scribbling some of the controlling techniques for inverters will be discussed as well. In this section the related works also will be discussed.

**Chapter 3** will address the theory and modeling of the PV system.

**Chapter 4** will describe the Simulink block used to model the PV system.

**Chapter 5** will give an example of PV system and analyze the results.

**Chapter 6** will conclude the report and future research.

**Chapter 7** will conclude references.

**Appendix**

## CHAPTER 2

### LITERATURE SURVEY

Nicholas Jenkins *et al.*[1], M.G.Villalva *et al.*[2], Huan-Liang Tsai *et al.*[3], I.H. Altas *et al.*[4] and Hasaneen, B.M. *et al.*[5] presented basic terminology regarding renewable energy that is solar energy.

Weiping Luo *et al.*[6], Antunes, F.L.M. *et al.*[7], R.Faranada *et al.*[8], Burkina Faso D Abdoulaye *et al.*[9] and Zhou Dejie *et al.*[10] proposed various methods for Tracking and controlling of maximum power point application in grid-connected photovoltaic generation system.

Liang Ma *et al.*[11] has presented solar grid system.

<http://www.mbipv.net.my> (Pusat Tenaga Malaysia) [12], <http://www.met.gov.my> (Jabatan Meteorologi)[13], <http://www.ieeeexplorer.com> [14] and [ecee.colorado.edu/~ecen2060/materials/lecture.../GridPVsystem.pdf](http://ecee.colorado.edu/~ecen2060/materials/lecture.../GridPVsystem.pdf) [15]

Muhammad H. Rashid *et al.*[16], Chetan Singh Solanki *et al.* [17] and R.W. Erickson *et al.*[18] worked on various topologies of tie line control.

Gwinyai Dzimanu *et al.*[19], Falinirina F. Rakotomananandro *et al.*[20], Suresh A/L Thanakodi *et al.*[21], David Sanz Morales *et al.*[22] and Akihiro Oi *et al.*[23] compared different techniques regarding tie-line control of grid solar system.

#### **2.1 Potential Energy of Photovoltaic System**

Through this chapter, hopefully it will give some idea to the reader regarding the different technologies of photovoltaic cells and different modeling techniques as well. Besides that, basic concepts regarding photovoltaic will be reviewed as well as the power electronics converters. On the other hand, the inverters and grid connected PV system also shall be discussed, Circuit Based Simulation of Photovoltaic Arrays [2].

In addition, related works regarding to this research project work also will be conferred in depth. It's an honor to be the medium of knowledge manifestation from the universe.

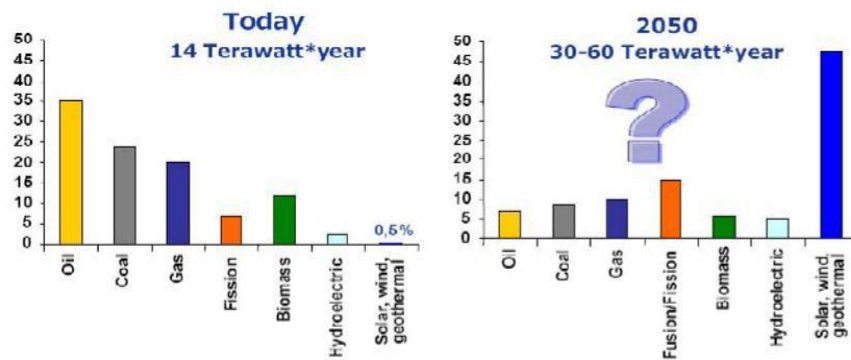


Fig. 2.1 Resources Energy Trend

From Fig. 2.1, it can clearly deduce that the natural sources are depleting in years to come and this eventually results on the cost of energy production. It can also clearly see the trend moves towards renewable energy especially on photovoltaic system. Hence, as a conclusion, the photovoltaic system can be the next best energy source.

## 2.2 Different technology of Photovoltaic's

There are many types of technology in thin film photovoltaic technology. For an example in this thin film technology there is Silicon based and Chalcogenide based cells. Table 2.1 shows the summary of the types that shall be discussed in this topic.

TABLE 2.1

SUMMARIZE THE DIFFERENT TECHNOLOGY IN THIN FILM TECHNOLOGY

Thin Film Technologies	
Silicon based	Chalcogenide-based cells
Single junction amorphous silicon	Cadmium Sulphite (CdS)
Multiple junction amorphous silicon	Cadmium Telluride (CdTe)
Crystalline Silicon on Glass	Copper Indium deselenide (CIS)



In the thin film technology it can be divided into two major parts which is silicon based and chalcogenide based. As for beginning look at silicon based which consists of single junction amorphous silicon, multiple junction amorphous silicon and crystalline silicon on glass. Below in Fig. 2.2 (a) is the single junction amorphous silicon and Fig. 2.2 (b) is the individual cells deposited onto a glass sheet are laterally connected in series by the approach shown.

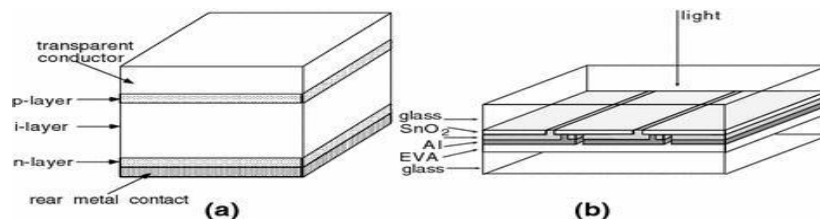


Fig. 2.2 (a) Single Jn. amorphous & (b): Cells connected in series

In the early 1980s the calculators and digital watches have been using the amorphous silicon solar. At that time, many efforts were carried out but currently Kaneka and Mitsubishi are the companies that successfully supplies single junction amorphous silicon. This is due to its characteristics that in the low temperature the amorphous silicon allows 10% hydrogen to be incorporated. Quality of the material is improved in the presence of the hydrogen atom. The amorphous silicon is not very conductive hence the transparent conductive tin oxide layer between the silicon and the glass being used and connected in series as depicted in Fig. 2.2(b)

The next is the multiple junction amorphous silicon devices, where it is designed in thinner layers to accommodate the decreased material quality under light exposure such as in single junction amorphous. It's made possible by stacking two or more cells on top of one and another as in Fig. 2.3. In effort to boost its performance the upper cells band gap is made larger compared to the lower cells.

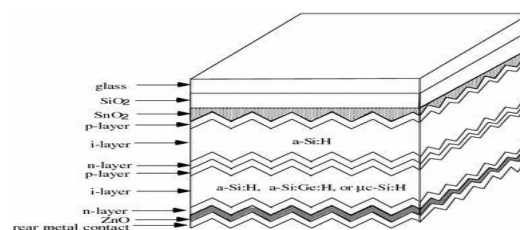


Fig. 2.3 Multiple-Jn. stacked or tandem solar cells where two or more current-matched cells are stacked on top of one another

By increasing the band gap of the upper cell there's a change in performance and the earliest effort made in reducing the band gap by alloying it with germanium. This result in the performance was around the 6–7% range, compared to the best of the single junction amorphous silicon (a-Si).currently there's another way of doing it whereby an a-Si as top cell combined with a bottom cell which consists a mixture of amorphous and microcrystalline as in Fig. 2.4. Another type of solar cell is crystalline silicon on glass as depicted in Fig. 2.5 whereby this technology uses high temperature to transform the amorphous silicon material to polycrystalline. This technology has some similarity with the polycrystalline wafer.

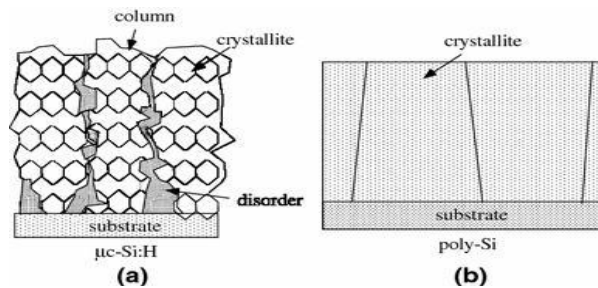


Fig. 2.4 (a): Mixed-phase microcrystalline/amorphous material & (b): Single-phase polycrystalline film.

The advantage of this technology is that the material is more conductive and there's no need for a transparent conducting oxide that results in cost reduction. The instability possessed by a-Si is also solved using this material. The glass texture is also another plus point in this technology as it allows the silicon layer to be very thin.

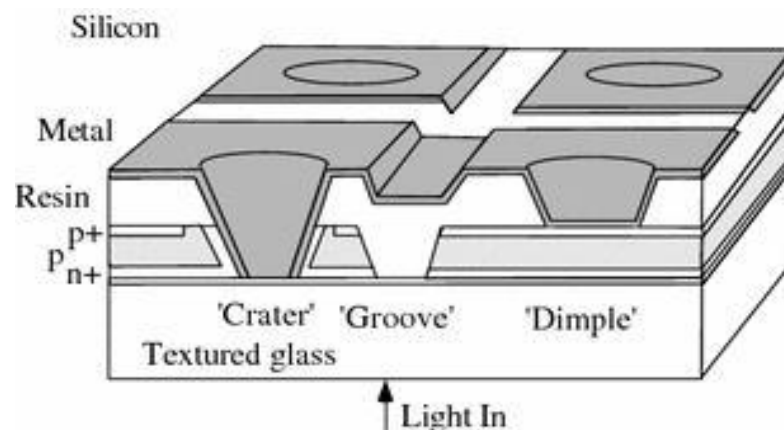


Fig. 2.5 Crystalline silicon on glass (CSG) unit cell structure.

Earlier the discussions were on the silicon based; now let's have a preview on the Chalcogenide-based cells [3]. The Chalcogenide-based cells kick off with the cadmium sulphite technology in the early 1980s. Yet this technology was beat down by the biggest contender at the time; amorphous silicon. Besides that, the instability issue with cadmium sulphite was another major issue. When the amorphous silicon was going thru dark ages as it had problem with commercialization, this technology had a good time and became famous.

BP solar and Matsushita were manufacturing Cadmium Telluride solar cell and then later move on to other technology due to environmental issues. The toxicity of cadmium was one of the reasons. A layer of cadmium sulphide is deposited from solution onto a glass sheet coated with a transparent conducting layer of tin oxide. This is followed by the deposition of the main cadmium telluride cell by as variety of techniques including close-spaced sublimation, vapour transport, chemical spraying, or electroplating. The cadmium telluride structure has been depicted in Fig. 2.6.

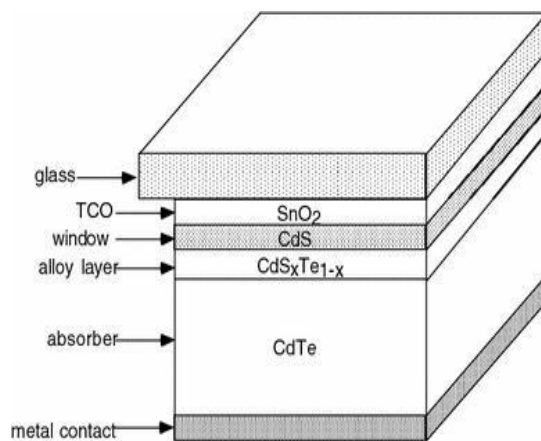


Fig. 2.6 Device schematic for a cadmium telluride cell

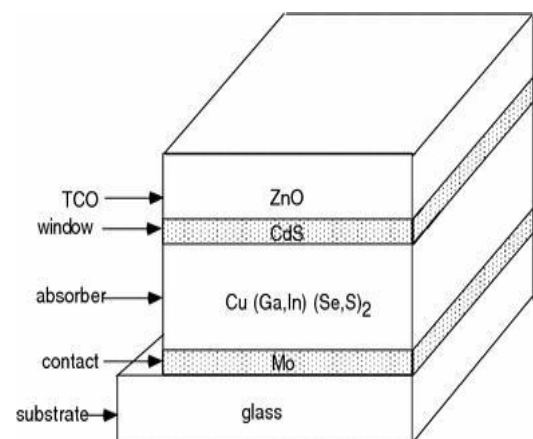


Fig. 2.7 Basic CIS (copper indium diselenide) cell structure

Copper Indium diselenide known as CIS technology has demonstrated 19.5% efficiency in experiments yet it's hard to commercialize. CIS technology generally involves deposition onto a glass substrate and then interconnected as in Fig. 2.7.

An additional glass top-cover is then laminated to the cell/substrate combination. Yet the CIS technology is one of available resources as reserves of indium would only produce enough solar cells to provide a capacity equal to all present wind generators.

TABLE 2.2

CONFIRMED TERRESTRIAL MODULE EFFICIENCIES MEASURED UNDER THE  
GLOBAL AM 1.5SPECTRUM

<b>Material</b>	<b>Efficiency</b>	<b>Voc</b>	<b>Ioc</b>	<b>Fill Factor (FF)</b>
Si (crystalline)	22.7± 0.6	5.6	3.93	80.3
Si (large crystalline)	20.1 ± 0.6	66.1	6.30	78.7
Si (multi crystalline)	15.3 ± 0.4	14.6	1.36	78.6
Si(thin-_lm polycrystalline)	8.2 ±0.2	25.0	0.328	68.0
CIS	19.5 ±0.7	31.2	2.16	68.9
CdTe (thin _lm)	10.7 ± 0.5	26.21	3.205	62.3

### 2.3 Electrical Equivalent of Solar Cells

Earlier in sub topic 2.2 the discussion were about types of solar cells in terms of materials, but in this sub topic the discussion will be on the solar cell equivalent electrical circuits and their mathematical equations in depth. Before going deep in the topic, let's have some basic on how the solar cell works [4].

As discussed earlier since the solar cell are made of specially treated silicon whereby positive (on the backside) while the negative part (facing the sun), when the sun light (radiation) hits the solar cell, the electrons gets excited and loose creating the electron-hole pairs.

This phenomena when extended by attaching the electrical wires on positive and negative part creating a close loop while then results in current flows which known as electric photocurrent (IPH). This is clearly shown in Fig. 2.8 courtesy of PV Industry Hand Book by PTM.

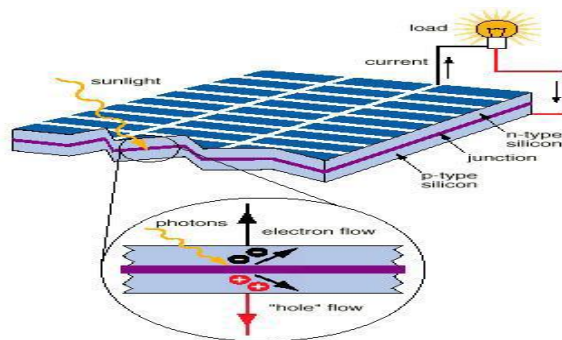


Fig. 2.8 Summary on how solar cells work

As for the kick start, the understanding on the operation and electrical equivalent circuit of single solar cell will be discussed. Referring to Fig. 2.9, without the sun light (dark), the solar cell shall function as a normal diode. If any external supply connects to it, the solar cell will function and produce the diode current ( $I_D$ ). In the dark, the solar cell will not produce any electric current or voltage.

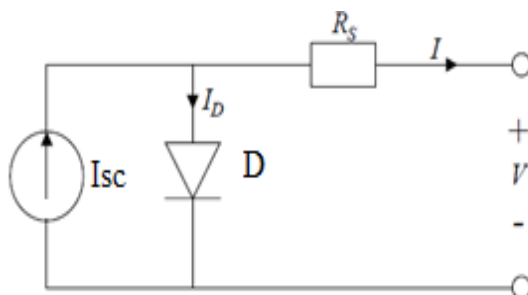


Fig. 2.9 Model for single solar cell

This solar cell model consists of a current source ( $I_{ph}$ ), series resistance ( $R_s$ ) which representing the resistance inside the each cell as well in the connection between the cells, and a diode. The difference between  $I_{ph}$  and  $I_D$  will give the net current output from the solar cell.

The mathematical equation can be represented as in equation 2.1. The equation is actually using Kirchhoff Current Law (KCL) and also diode Shockley equation. The  $m$  is the representation of idealizing factor,  $k$  Boltzmann's gas constant,  $T_c$  will be absolute temperature of the cell,  $e$  will be electric charge, and  $V$  will be the voltage implied across the cell.  $I_0$  is saturation current in dark surroundings and depends on the temperature.

$$I = I_{ph} - I_D = I_{ph} - I_0 \left( \exp \frac{e(V + IR_s)}{mkT_c} - 1 \right) \quad (2.1)$$

The solar cell has certain parameters, such as short circuit current, open circuit voltage, maximum power point, maximum efficiency, and fill factor. Short circuit current is the best current produced when the solar cell under short circuited situation which means the voltage as zero. In other word  $I_{sc} = I_{ph}$ . Then another parameter of solar cell is open circuit voltage. This open circuit voltage can be obtained during night time (dark) whereby the current produced is zero and related to voltage drop across the diode.

It can also represented by mathematical equation such as in equation 2.2 whereby  $\frac{mkT_c}{e}$  is known as thermal voltage and  $T_c$  is the absolute cell temperature.

$$V_{oc} = \frac{mkT_c}{e} \ln \left( \frac{I_{ph}}{I_0} \right) = V_t \ln \left( \frac{I_{ph}}{I_0} \right) \quad (2.2)$$

Maximum power point is another parameter that being used in the solar cell operation whereby it states the maximum power dissipated at the load. Referring to Fig. 2.9 courtesy from Model for Stand Alone PV system by Anca D Hansen, the maximum operating point is depicted in the said Fig.2.10

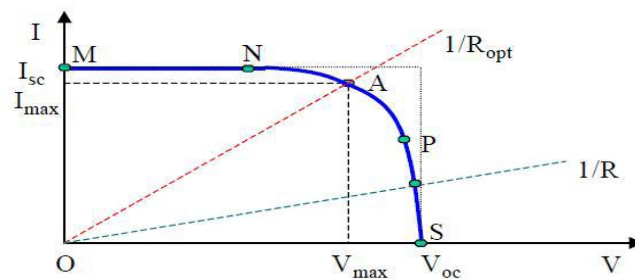


Fig. 2.10 A typical current-voltage ( $I$ - $V$ ) curve for a solar cell.

Maximum efficiency is another parameter for solar cell need to be considered as well. Maximum efficiency in the solar cell context means the ratio between incident light power and maximum power. The equation 2.3 depicts clearly and as  $G_a$  is the ambient irradiation as well the  $A$  is the cell area.

$$\eta = \frac{P_{max}}{P_{in}} = \frac{I_{max} \cdot V_{max}}{A \cdot G_a} \quad (2.3)$$

Fill factor (FF) is another parameter used in the solar cell analysis. Fill factor can be defined as how close the  $I$ - $V$  curve can get close to be a square wave. Another definition of fill factor is the ratio of maximum power that can be delivered to the load compared to  $I_{sc}$  and  $V_{oc}$ . In equation 2.4, the formula is shown clearly.

$$FF = \frac{P_{max}}{V_{oc} I_{sc}} = \frac{V_{max} I_{max}}{V_{oc} I_{sc}} \quad (2.4)$$

The PV system normally uses solar panels, which is in arrays. There are many types of PV system, starting from a cell up to arrays. This is shown in Fig. 2.11

In ensuring protection for solar cells and electrical connectors from the raging environment the cells were grouped together into ‘modules’ As depicted in Fig. 2.12, the manufacturer normally supplies the module with  $N_{pm}$  (number of parallel module) and in the each branch with  $N_{sm}$  (number of cells in series).

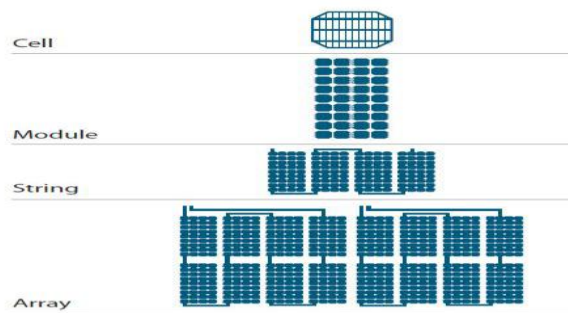


Fig. 2.11 The PV from cell to module

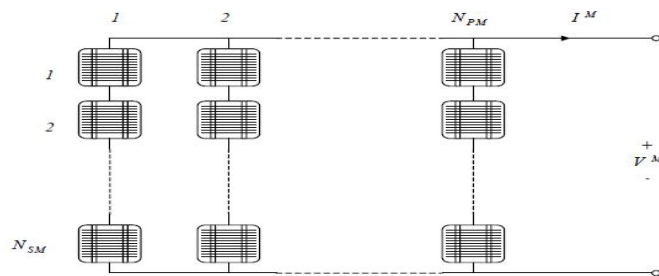


Fig. 2.12 PV module consists of parallel and series cells

As shown in Fig. 2.13, the PV modules in Fig. 2.12 now are connected in arrays. Fig. 2.13 clearly shows that an array with  $M_p$  (module in parallel) parallel branches each with  $M_s$  (module in series) [5].

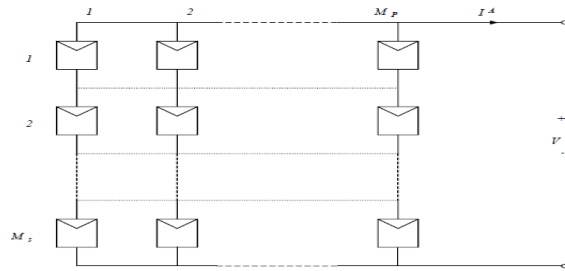


Fig. 2.13 Solar cells array consist of  $M_p$  parallel branches each with  $M_s$  Modules in series

The arrangement of the module is also plays a big role in terms of efficiency. In the Fig. 2.14, show different types of module connection. The A configuration have demonstrated efficiency up to 97.2% while configuration B efficiency at 96.8% and C at 96.2%.

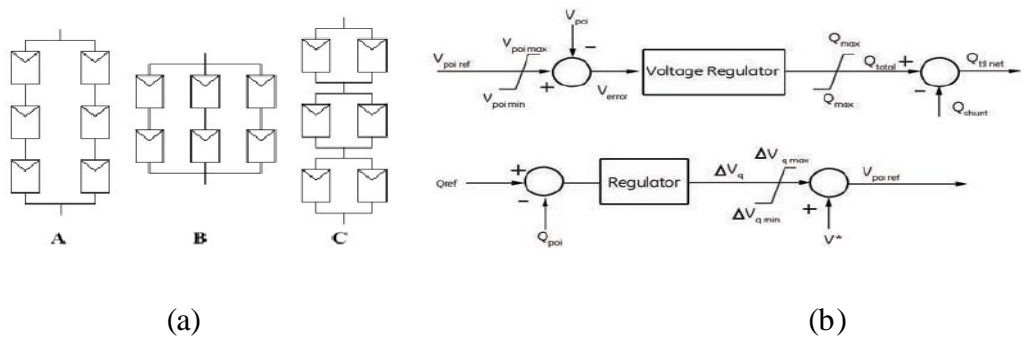


Fig. 2.14 (a) Series-parallel configuration for PV generator & (b) M-VAR Block Diagram

TABLE 2.3

COMPARISON BETWEEN DIFFERENT CONNECTION TOPOLOGIES OF PV SYSTEMS

Topology	Advantages	Disadvantages	Power rating
Centralized	1- Easy to monitor 2- Easy to maintain 3- low cost due to central inverter	1- DC losses in high voltage DC cables 2- Power loss due to centralized MPPT, string diodes and mismatch in PV	up to several megawatts



		modules 3- Low reliability 4- Not flexible in design	
Master-Slave	1- Higher reliability as compared to centralized topology 2- Improved efficiency for the operating inverters 3- Extended lifetime of inverters	1- DC losses in high voltage DC cables 2- Power loss due to centralized MPPT, string diodes and mismatch in PV modules 3- High cost due to use of multiple inverters 4- not flexible in design	up to several megawatts
String	1- Reduction in energy loss that result from partial shading 2- Losses in string diodes are eliminated 3- Good reliability 4- Flexible in the design	1- Higher cost as compared to centralized 2- Used for low power ratings	3-5 kW / String
Multi-String	1- Reduction in energy loss that result from partial shading 2- Losses in string diodes are eliminated 3- MPPT and current control are separated 4- Voltage amplification can be achieved by the DC-DC converter	1- All strings are connected to a single inverter thus the reliability of the system decreases 2- Additional losses inside the DC/DC converter 3- The cost is higher as compared to centralized topology	5 kW
AC Modules	1- No losses due to partial shading 2- No mismatch losses between modules 3- Easy in failure detection of the modules 4- Flexible & expandable in design	1- High cost 2- Replacement of inverter in case of faults is not easy 3- Reduced lifetime of the power electronic components due to Additional thermal stress	up to 500 W

Photovoltaic systems have become an energy generator for a wide range of applications. The applications could be standalone PV systems or grid connected PV systems. A standalone PV system is used in isolated applications where PV is connected directly to the load and storage system. With a standalone photovoltaic, when the PV source of energy is very large, having energy storage is beneficial. Where as a PV system that is connected through a grid is used when a PV system injects the current directly into the grid itself [5]. The advantage of the grid-connected system is the ability to sell excess of energy.

### **2.3.1 The other benefits are:**

“Mitigation of short-term solar power intermittency and wind gust effects and minimizing its impacts on voltage, frequency, and power fluctuations in power system”

“Lowering the transmission and distribution costs by increasing the confidence in renewable distributed generation”

Improving power system stability, reduction of harmonics,

### **2.3.2 Tie-line Control Design:**

A “tie line” refers to the feeder connection between the Micro-grid and bulk grid. Tie-line controls can be designed to manage the feeder power flow and voltage at the point of interconnection (POI) to meet the needs of the system operator. Control is implemented by coordinating the assets of the Micro-grid, allowing the collection of these assets to appear as one aggregated dispatch able producing or consuming entity connected to the bulk grid. This section outlines the reactive and active power controls required for this capability.

#### **Micro grid Reactive Power Control (M-VAR)**

The primary functions of M-VAR are voltage regulation and power factor control at the tie-line. Capabilities include voltage set point, steady state voltage response, and transient VAR response. The M-VAR controller can receive either an external remote reactive power command or a voltage command from the system operator. The closed loop control issues reference VAR commands over the communication channel to each Micro grid controllable asset controller. The local controls ultimately are responsible for regulating the VARs locally in each component. The controller compares the VAR output at the tie-line or point of

terconnection (POI) and adjusts the M-VAR command to obtain the desired system voltage. M-VAR control has two modes of operation: voltage regulated and VAR regulated (Fig. 2.14 b). The voltage  $V_{poi}$  refers to the measured line-to-line RMS value.  $Q_{poi}$  is to the total reactive power measured at the POI. In the voltage regulation mode, the voltage error is compensated by a proportional-integral (PI) controller to produce a total reactive power demand [6]. After subtracting the shunt reactive power, provided by the shunt capacitors (if any), the total reactive power command,  $Q_{ttl, net}$ , for the controllable asset in the Micro-grid is obtained.

In the VAR regulation mode, the error between the  $Q$  reference and the  $Q$  measurement at the POI is regulated by a PI regulator. By adding the desired voltage feed forward, it provides a voltage reference to the voltage regulation loop. The total reactive power command is applied to the dispatch reference selection function to generate a reactive power command for each individual available controllable asset.

## 2.4 Grid Connected PV System

A grid connected PV system also known as utility interactive PV system, whereby it feed solar electricity directly to a utility power grid. For a general knowledge about we are discussing, kindly refer to Fig. 2.15.

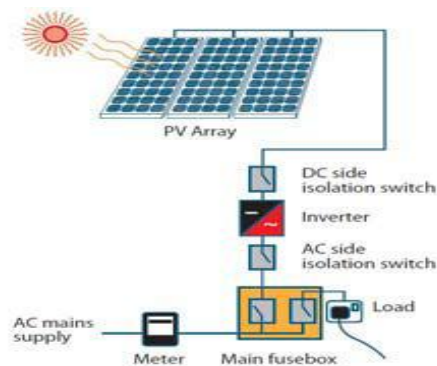


Fig. 2.15: Grid-connected PV System

This grid connected PV System, consists of a PV Generated, an array of PV modules converting solar energy to DC electricity and an inverter also known as a power conditioning unit that converts direct current generated by PV to alternating current for the grid usage. Surge protector and load are also the grid-connected PV components. When the sun shines,

the DC power generated by the PV modules is converted to AC electricity by the inverter. This AC electrical power can either be supply the system's AC load and the excess energy output transmit to the utility grid. Fig. 2.16 will give basically the detail component about the grid connected PV system.

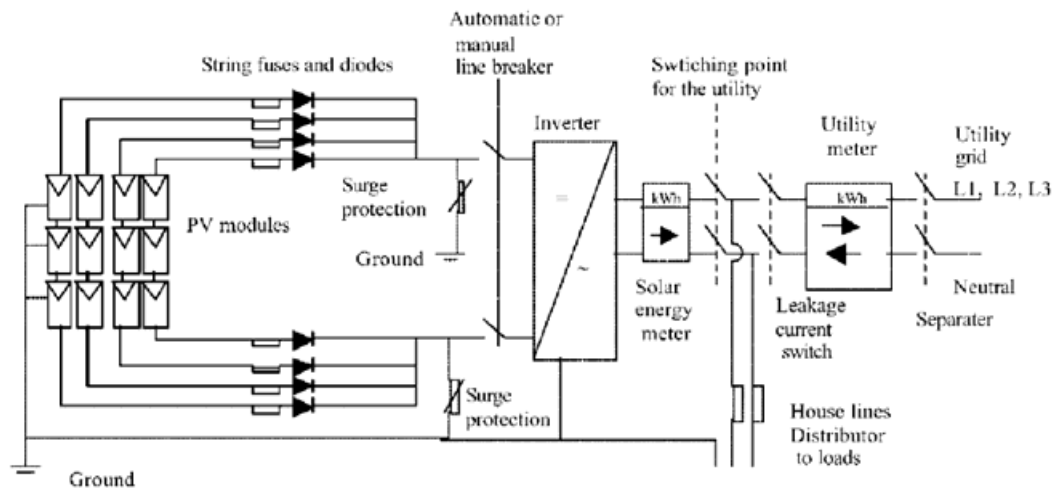


Fig. 2.16 A detailed Grid-Connected PV System

Referring to Fig. 2.16, a first protection level is formed by fuses and blocking diodes between the PV array output and the main DC conductor. Surge protection elements have to be included at the inverter input and output as well. The grid-connected PV system can be classified by its sizing whereby from 1-10kWh is considered as small scale and normally for the domestic usages. While medium size is defined from 10kWh to 100kWh and these kind of system is known as building integrated PV (BIPV). The system with output of 500kWh – MWh is considered as large size and normally operated by electric companies.

## 2.5 Solar Cell and its Characteristics

This subtopic will be discussing in depth about the solar cell and its characteristics. The I-V curve, crucial parameters from manufacturer's datasheet, effect on the I-V curve when there's change on solar radiation and temperature as well the mathematical equation used for modeling in this project shall be discussed in this subtopic which will help to have deeper understanding in verifying the solar modeling later part of the project.

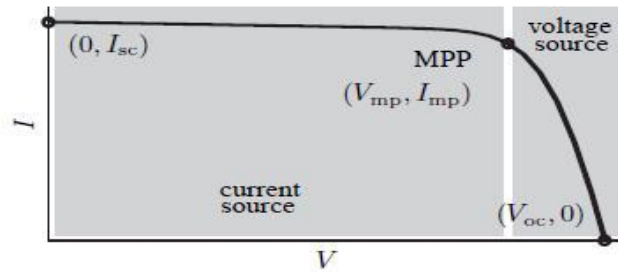


Fig. 2.17 Characteristic  $I$ - $V$  curve of a practical photovoltaic device

Fig. 2.17, depicting the solar cell  $I$ - $V$  curve of a practical photovoltaic device where it is clearly notice that when voltage is short circuit, the short circuit current ( $I_{sc}$ ) happens and also practically given in the manufacturer’s data sheet. On the other hand when the circuit is open, there’s no current flow and the point is known as the open voltage ( $V_{oc}$ ) also given by the manufacturer’s datasheet [6]. Another parameter also available to us thru the data sheet is the maximum current and voltage point. These three main points will be used later part in verifying our modeling.

For a solar cell, the non-linear relationship means the maximum power point has to be determined by calculating the product of the voltage and output current. In order to extract maximum power from the solar cell, the solar cell must always be operated at or very close to where the product of the voltage and output current is the highest. This point is referred to as the maximum power point (MPP), and it is located around the ‘bend’ or ‘knee’ of the  $I$ - $V$  characteristic [13].

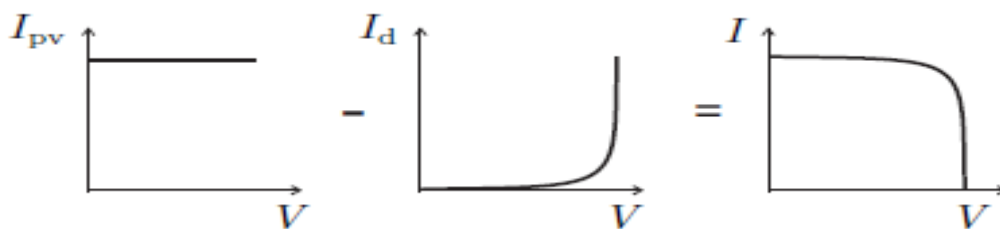


Fig.

2.18 Characteristic  $I$ - $V$  curve of the photovoltaic cell

From Fig. 2.18 it can be concluded that photovoltaic is a non-linear device and using Fig. 2.19 a great height of understanding can be achieved as the  $I_{pv}$  is the light generated current and the  $I_d$  is the diode current and  $I$  is the net cell current composing both  $I_{pv}$  and  $I_d$ .

Referring to Fig. 2.17, it can also be understood that from the operating characteristic of a solar cell consists of two regions: the current source region, and the voltage source region. Whereby in the current source region, the internal impedance of the solar cell is high and this region is located on the left side of the current-voltage curve (0,  $I_{sc}$ ).

While the voltage source region, where the internal impedance is low, is located on the right side of the current-voltage curve ( $V_{oc}$ , 0). As can be observed from the characteristic curve, in the current source region, the output current remains almost constant as the terminal voltage changes and in the voltage source region, the terminal voltage varies only minimally over a wide range of output current.

According to the maximum power transfer theory, the power delivered to the load is maximum when the source internal impedance matches the load impedance. For the system to operate at or close to the maximum power point (MPP) of the solar panel, the impedance seen from the input of the maximum power point tracker needs to match the internal impedance of the solar panel. Although controlling these points can produce a better voltage yield yet, the temperature and solar radiation is just unpredictable. That's another reason why many research are being also conduct to have smart solar system.



Fig. 2.19(a): Characteristic shown on the influence of ambient irradiation [15] &

Fig. 2.19(b): Characteristic shown on the influence of cell temperature [15]

When the solar radiation changes the current produced is also change accordingly for an example when the solar radiation increase, clearly from Fig. 2.19(a) clearly depicts that the short circuit current will increase and vice versa[7]. Fig. 2.19(b) shows the response from solar cell when there's a change on the temperature. When the cell temperature decreases the open circuit voltage shifts to a lower voltage and thus the changes in solar radiation and

temperature shifts the maximum power point operation, which can influence the overall performance [8]. Thru this Fig. 2.19(a) and (b), it can be concluded that solar radiation and cell temperature are two most important parameters that should be considered while modeling the photovoltaic.

Normally in the practical world, solar cell can be connected in many different manner as discussed earlier it can be connected in series or parallel. Fig. 2.20 shows the responses on the  $I$ - $V$  curves when the two identical cells are connected in series and in parallel. Referring to Fig. 2.20, for a series connection, the voltage would be increased and the analysis would be adding the voltages for each current, while for parallel connection, current of each individual cell can be add up at each voltage in order to arrive at the same response as depicted in Fig. 2.20.



Fig. 2.20 (a): The  $I$ - $V$  curve responses with two identical cells connected in series &

Fig. 2.20 (b): The  $I$ - $V$  curve responses with two identical cells connected in parallel

As the discussion on the solar cell characteristics and also on how the surroundings factor effect on the solar cell have come to an end. It would be very helpful in modeling and verification if the right understanding about standard testing condition well known as STC in reading the manufactures' data sheet is understood. STC conditions known as the reference vertical irradiance  $E_0$  with a typical value of  $1000\text{W}/\text{m}^2$ , the cell's reference temperature for performance rating,  $T_0$  with a typical value of  $25^\circ\text{C}$  and a tolerance of  $\pm 2^\circ\text{C}$ ; and a specified light spectral distribution with an air mass,  $AM = 1.5$ . The air mass (AM) Fig. provides a relative measure of the path the sun must travel through the atmosphere. Furthermore in supplying the performance parameters at the Standard Test Conditions manufacturers also provide performance data under the Nominal Operating Cell Temperature (NOCT). This is known as the temperature reached by the open circuited cells in a module under the following conditions:

Irradiance on cell surface is  $800\text{W/m}^2$

The ambient temperature is  $20\text{ }^\circ\text{C}$  ( $293\text{ K}$ )

Wind speed is  $1\text{ m/s}$  with the mounting is open back side

According to Evans, 1981 formula the cell temperature  $T_c$  ( $^\circ\text{C}$ ) is related to the mean monthly ambient temperature,  $T_a$  ( $^\circ\text{C}$ ) and this formula will be used in this project to as a parameter input, and given in the expression below.

$$T_c + T_a = (219 + 832 \frac{\overline{K_t}}{800}) (\frac{NOCT - 20}{800}) \quad (2.5)$$

Where (NOCT) is the Nominal Operating Cell Temperature and  $\overline{K_t}$  is the monthly clearness index (range between 0.2 for a very overcast climate and 0.8 for a very sunny climate).

As for familiarization, Fig. 2.21 is taken from Sharp NE-80EJEA solar cell which depicting its electrical characteristics and the important parameter that need to be used during the modeling time for an example number of cells and the connection type This literature will come in handy to understand the modeling process in Chapter 3 later on. Besides that Fig. 2.22 also were included in order to familiar the reader with the  $I$ - $V$  curve [8], and these is the type of graph from manufacturer which will be helpful during verification process after the modeling. The  $I$ - $V$  curve clearly also shows to us on how the solar radiation will play its role in the current generated from the solar cells.

ELECTRICAL CHARACTERISTICS	
Cell	Poly-crystalline silicon
No. of Cells and Connections	36 in series
Open Circuit Voltage (Voc)	21.6V
Maximum Power Voltage (Vpm)	17.3V
Short Circuit Current (Isc)	5.16A
Maximum Power Current (Ipm)	4.63A
Maximum Power (Pmax)*	80W (+10% / -5%)
Module Efficiency ( $\eta_m$ )	12.40%
Maximum System Voltage	600VDC
Series Fuse Rating	10A
Type of Output Terminal	Junction Box

Fig. 2.21: Electrical characteristics of Sharp NE-80EJEA solar cell

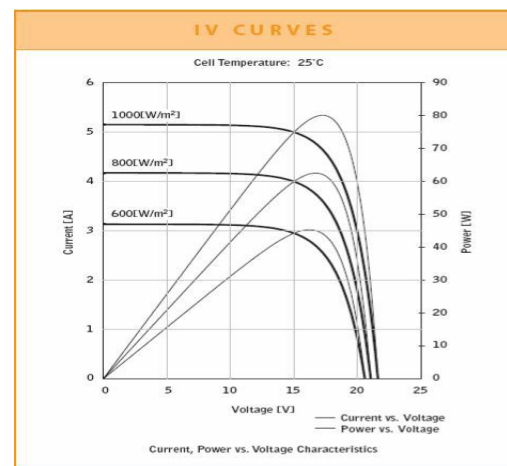


Fig. 2.22 Electrical characteristics of Sharp NE-80EJEA solar cell



The efficiency,  $\eta$  of the solar module is another crucial criterion that needs to consider before selecting the module. This efficiency mostly influence by the temperature. The equation of the efficiency and energy of the solar module are shown as following and Table 2.2 shows to us the PV module characteristics for standard technologies.

$$\eta_p = \eta_r * [1 - \beta_p] \quad (2.6)$$

TABLE 2.4

PV MODULE CHARACTERISTIC FOR STANDARD TECHNOLOGIES

<b>PV module type</b>	<b><math>\eta_r</math> (%)</b>	<b>NOCT (°C)</b>	<b><math>\beta_p</math>(% / °C)</b>
Mono-Si	13.0	45	0.40
Poly-Si	11.0	45	0.4
a-Si	5.0	50	0.11
CdTe	7.0	46	0.24
CIS	7.5	47	0.46

In order to determine the effectiveness of PV system the efficiency of the PV module plays a big role. There's plenty of factor that can affect the efficiency of the PV system such as natural climatic conditions of the place where the system is to be used, optimal matching of the system with the load, appropriate spatial placement of the modules (placing the modules at an optimal inclination angle to the horizontal plane) and availability of a concentrator (reflector) and or solar tracking mechanism in the system.

This project will emphasize more on the energy delivered by the PV array,  $E_p$ , and energy that available to the load  $E_a$ . As both these parameter are given by the formula as in equation 2.7 and equation 2.8. In addition to that, as the energy pass thru the inverter there will some losses depending on the inverter's efficiency which is given by the equation 2.9 and after the energy travel thru the grid, there will be some energy absorption in the grid that need to be considered which is given in the equation 2.10.

$$E_p = \eta_p (A * \overline{Ht}) \quad (2.7)$$

$$E_A = E_p (1 - \lambda_p) (1 - \lambda_c) \quad (2.8)$$

$$E_{grid} = E_A * \eta_{inv} \quad (2.9)$$

$$E_{dlvd} = E_{grid} * \eta_{inv} \quad (2.10)$$

## 2.6 Converters and Inverters

The rise of power electronics in the industry have always been a factor for the growth in the PV system. As for that, this literature review will be incomplete without the power electronic discussion. As gratitude and to pay some tribute for the works done in the power electronic world some basic power electronics shall be covered here. The role of power electronic converters is to provide power to the user in a suitable form at high efficiency [9]. Power electronic converters are needed in PV systems to convert direct current (DC) voltage to the required values and to convert from DC to alternating current (AC) and vice versa. In addition they control the charging and discharging of batteries in systems where batteries are storage elements especially for the standalone PV system.

One of the simplest power electronics circuits is the buck converter and basically consists of an inductor, a power electronic switch (usually a MOSFET or an IGBT) and a diode. It may have a capacitor to smooth the output. Its function is to step down DC voltage as depicted in Fig. 2.23.

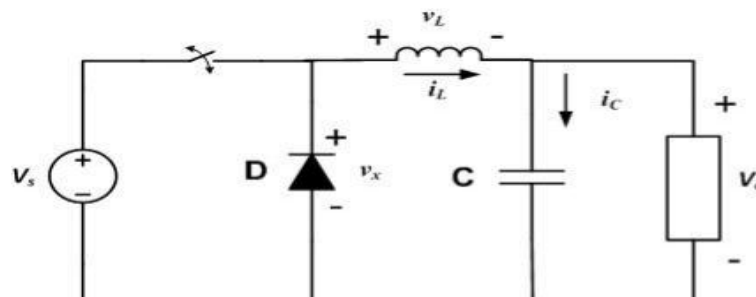


Fig. 2.23: The Schematic of a Buck Converter [18]

If the switch is turned on and off repeatedly at very high frequencies (10kHz! 100MHz) and assuming that in the steady state the output will be periodical then:

$$v_o(t + T) = v_o \quad (2.11)$$

$$i_o(t + T) = i_o \quad (2.12)$$

The current in the load is given by  $I_R = V_o/R$ . The average DC component of the capacitor current must be equal to zero otherwise the capacitor voltage will be increasing and there will be no periodic steady state. If the switch is turned on and off repeatedly at very high frequencies such as 10kHz to 100MHz and assuming that in the steady state the output will be periodical then:

$$\langle I_c \rangle = I_c = 0$$

$$\langle i_L \rangle = I_L = I_R = \frac{V_o}{R} \quad (2.13)$$

Likewise the DC component of voltage across the inductor has to be zero:

$$\langle v_L \rangle = \frac{1}{T} \int v_L dt = 0 \quad (2.14)$$

The duty ratio  $D$  is defined as the fraction of the switch period during which the switch is on given by:

$$D = \frac{t_{on}}{T} \quad (2.15)$$

The average voltage across the inductor will be given by:

$$\begin{aligned} \langle v_L \rangle &= \frac{1}{T} \left( \int_{0}^{DT} v_{on} dt + \int_{DT}^{(1-D)T} v_{off} dt \right) \\ &= \frac{1}{T} \left( \int_{0}^{DT} (V_s - V_o) dt + \int_{DT}^{(1-D)T} -V_o dt \right) \\ &= \frac{1}{T} [(V_s - V_o) DT + (-V_o)(1 - D) T] \\ &= \frac{1}{T} (V_s DT - V_o T) \\ &= V_s D - V_o \\ &= 0 \end{aligned} \quad (2.16)$$

After solving we will get:

$$\frac{V_o}{V_s} = D \quad (2.17)$$

It can be seen that the output voltage is always less than or equal to the input voltage ( $0 \leq D \leq 1$ ). The converter may operate in the continuous conduction mode CCM or the discontinuous conduction mode DCM. In the CCM the inductor current is always greater than zero while in the DCM the inductor current is zero during certain portions of the switching period. In some applications both modes may be mixed. The filter inductor that determines the boundary is given by:

$$L_{\text{boundary}} = \frac{(1 - D)R}{2f} \quad (2.18)$$

Typically  $D = 0.5$ ,  $R = 10$ , and  $f = 100$  kHz, the boundary is  $L_b = 25\mu\text{H}$  [18]. Thus for any inductance larger than this value the buck converter will operate in the continuous conduction mode. In order to limit the ripple across the dc output voltage  $V_o$  to a value below a specific value  $V_r$ , the filter capacitance  $C$  must be greater than in the equation 2.19. The key design for buck mainly lies in the equation 2.18 and equation 2.19.

$$C_{\text{min}} = \frac{(1 - D)V_o}{8V_r L f^2} \quad (2.19)$$

Next we will view on the inverter, inverter is basically quite famous and a hot topic in the world of power electronics. In PV world, inverter plays a key point role as it's efficiency is also taken into accountability for the success of PV system. Due to the PV output is in DC form, the inverter will convert the DC to AC current. The inverter is characterized by the power dependant efficiency. Inverter plays the important role by keeping the voltage on AC side constant as well to perform power conversion from the input to output at efficient rate. The formula is given by equation 2.20.

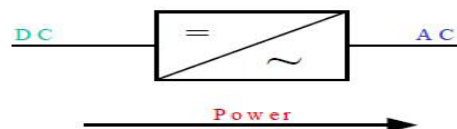


Fig. 2.24 Connection of Inverter

$$\eta = \frac{P_{out}}{P_{in}} = \frac{V_{ac} I_{ac} \cos \theta}{V_{dc} I_{dc}} \ggg I_{dc} = \frac{V_{ac} I_{ac} \cos \theta}{\eta V_{dc}} \quad (2.20)$$

There many inverters topologies, from three levels up to multilevel inverters are there for usage and there are also several topologies exist for both single phase and multi-phase inverters. For an example is a full bridge single phase inverter shown in Fig. 2.25. It consists of four switches that are turned is such a way that within a branch the upper and lower switches are never on at the same time to avoid short circuiting the DC source.

The inverter consists of four defined states and one undefined state as shown in Table 2.5. There are plenty of modulating techniques can be used to control the switching of the inverter switches but one common rule for all of them must avoid the undefined state and the short circuit conditions.

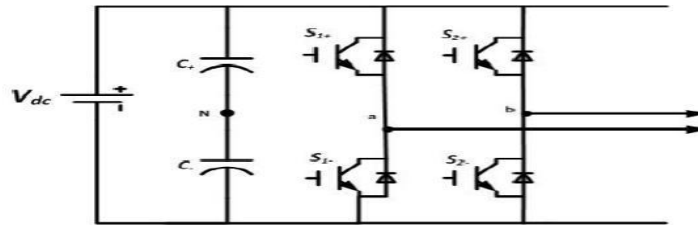


Fig. 2.25 Full Bridge Voltage Source Inverter

There are two general types of inverters namely, square wave inverters (line frequency switching) and pulse width modulation PWM inverters (high frequency switching) depending on the switching techniques used [10].

TABLE 2.5

THE SWITCHES STATE FOR A FULL BRIDGE SINGLE PHASE INVERTERS

State	Switch States	V <sub>an</sub>	V <sub>bn</sub>	V <sub>o</sub>
1	S1+ and S2- are on and S1- and S2+ are off	V <sub>dc</sub> / 2	-V <sub>dc</sub> / 2	V <sub>dc</sub>
2	S1+ and S2+ are on and S1- and S2- are off	-V <sub>dc</sub> / 2	V <sub>dc</sub> / 2	-V <sub>dc</sub>
3	S1+ and S2+ are on and S1- and S2- are off	V <sub>dc</sub> / 2	V <sub>dc</sub> / 2	0
4	S1- and S2- are on and S1+ and S are off	-V <sub>dc</sub> / 2	-V <sub>dc</sub> / 2	0
5	S1-, S1+, S2- and S2+ are all off	-V <sub>dc</sub> / 2	V <sub>dc</sub> / 2	- V <sub>dc</sub>

The norm practice to avoid the short circuit condition is by a very small time interval must be inserted between the turning off one switch and turning on the other. This short time interval time is referred to as the blanking time and largely depends on the type of semiconductor switch employed.

## CHAPTER 3

# SYSTEM DESCRIPTION AND MODELING OF THE PHOTOVOLTAIC SYSTEM

### 3.1 General topology of photovoltaic system

The MATLAB/SIMULINK software will be used for the modeling and simulation purposes. This software prepares all the electrical and mathematical blocks that needed in the project under Power System Block set, Signal Routing and Math Operations (Simulink). This software is easy to use as it is more on graphical user interface pertaining to building or modeling any circuits or mathematical equations.

Through this chapter, hopefully the reader will be able to grasp some idea on the usage of MATLAB/SIMULINK software. In addition, the method and steps in modeling the solar cell up to PV array are shown clearly. The first stage was modeling the mathematical equation for the Shockley diode current and the light generated photovoltaic current and later part will be extended for the array model.

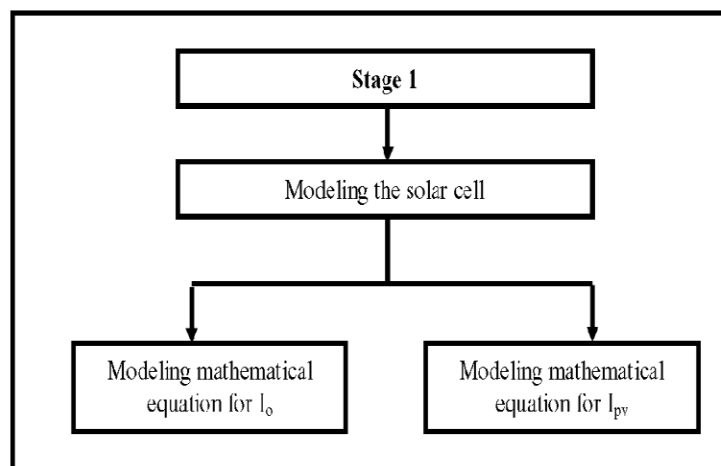


Fig. 3.1 First stage in modeling the solar cell

In the single stage configuration, as shown in Fig. 3.2, the interface of the PV array to the grid is realized with the DC/AC inverter [11]. The DC/AC inverter functions are to boost the PV voltage, track the MPP of the PV array and control the current injected to the grid.

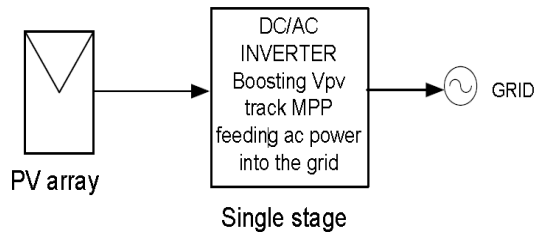


Fig. 3.2 Structure of Single stage DC/AC Photovoltaic system

In the other side, the dual stage configuration represented in Fig. 3.3 is composed of the DC/DC and DC/AC inverter to connect the PV array to the grid.

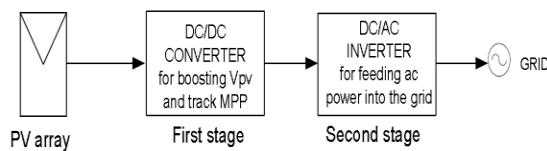


Fig. 3.3 Structure of dual stage DC/DC and DC/AC Photovoltaic system

The topology study in this thesis will be a photovoltaic linked with a converter focusing on the boost along with a resistive load. A boost converter with a controller for the maximum power point, which is used to track the MPP of the PV. This topology is shown in Fig. 3.4. It allows studying the efficiency of the maximum power point control method and the performance of the PV to achieve the maximum power at different temperature, irradiance and load.

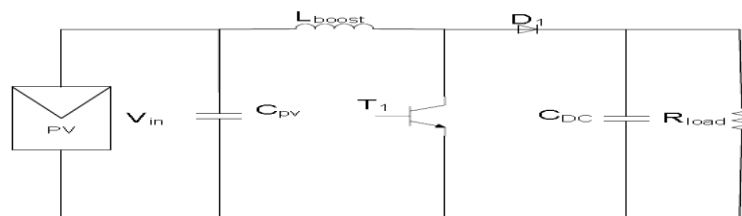


Fig. 3.4 Topology of PV with boost converter and resistive load.

Fig. 3.5 is a three-phase photovoltaic system with resistive load. In this topology, the photovoltaic array is the source of energy, the DC/DC boost converter is to adjust the DC-link voltage, tracks the maximum power and boost the PV voltage; the DC/AC inverter injects the AC currents to the load.



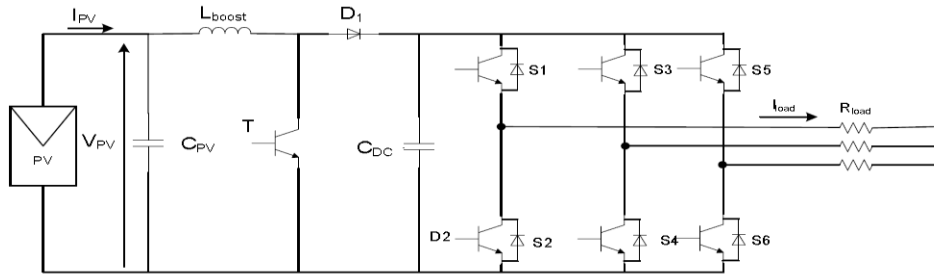


Fig. 3.5 Topology dual stage three-phase photovoltaic system with resistive load

### 3.2 Photovoltaic array modeling

#### 3.2.1 Curves I-V Characteristics of the PV array

Fig. 3.6 and 3.7 show the current voltage (I-V) characteristics of PV panel. This curve is nonlinear and crucially relies on the temperature along with the solar irradiation. In Fig. 3.6, when the irradiation increases [11], the current increases more than the voltage and the power maximum power point  $P_{mpp}$  increases as well.

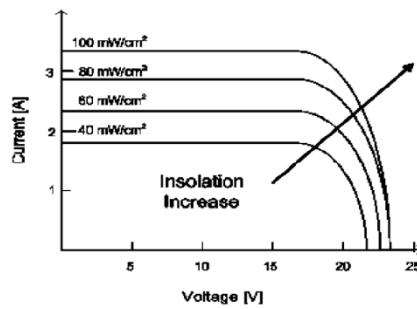


Fig. 3.6 I-V Characteristics of the PV as function of irradiance

Fig. 3.7 shows the variation of the current with the temperature, the current changes less than the voltage.

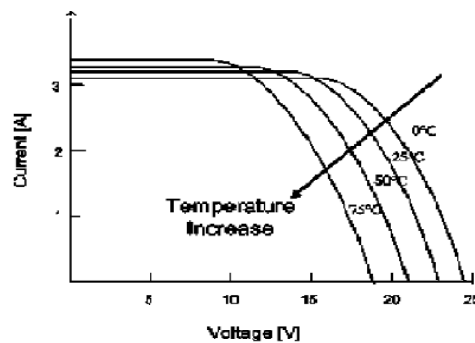


Fig. 3.7: I-V Characteristics of the PV as function of Temperature

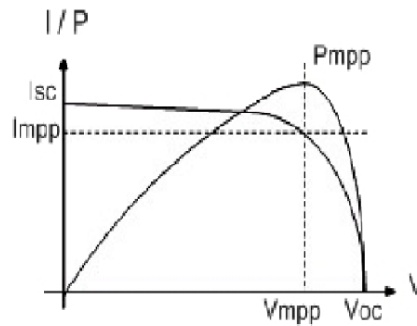


Fig. 3.8 I-V curve, P-V curve with the MPP

### 3.2.2 Model of the PV cell

PV cell is a semiconductor p-n junction that transforms sunlight to electrical power. To model a solar cell, it is imperative that we assess the effect of different factors on the solar panels and to consider the characteristics given by the manufacturers in the datasheet. It is to be noted that to form a PV module, a set of cells are connected in series or in parallel. To form a PV array, a set of PV modules are connected in series and in parallel. Thus, the mathematical models for PV array are attained while utilizing the basic description equivalent circuit of the PV cells.

A PV cell is usually embodied by an electrical equivalent of one-diode, resistance series  $R_s$  and resistance parallel  $R_p$  as shown in Fig. 3.9.

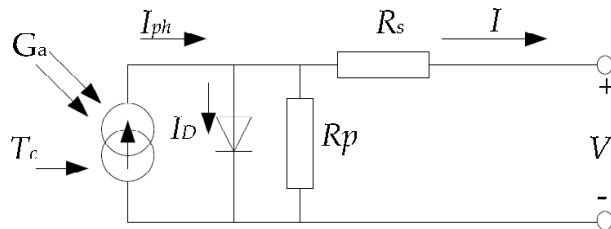


Fig. 3.9 Equivalent circuit of solar cell with one diode

From the Fig. 3.9, the different parameters characteristics of the PV cells are:

Manufacturer of the solar module gives other parameters needed to model the solar cells. The datasheet which gives the electrical characteristics is calculated under standard test condition STC when the temperature  $T$  is  $25^\circ\text{C}$  and the irradiance  $G$  is  $1000 \text{ W/m}^2$ . The parameters that

The solar cell is model first, then extends the model to a PV module, and finally models the PV array. From Fig. 3.6, the output current of the PV cell is given below.

$$I = I_{PH} - I_d \quad (3.1)$$

By Shockley equation, the diode current  $I_d$  is given by

$$I_d = I_0 \left( e^{\frac{qV_d}{kT}} - 1 \right) \quad (3.2)$$

The relation between voltage and current result by replacing the diode current

$$I = I_{ph} - I_0 \left( e^{\frac{qV_d}{kT}} - 1 \right) \quad (3.3)$$

Where  $V_d$  is the output voltage of the PV cell.

The reverse saturation  $I_0$  is found by using the above equation. By setting the current  $I$  equal to zero and calculating at temperature  $T_1$

$$I_0 (T_1) = \frac{I_{ph}(T_1)}{\left( e^{\frac{qV_d}{kT}} - 1 \right)} \quad (3.4)$$

The current generated by the solar cells  $I_{ph}$  can be approximated with the short circuit current  $I_{sc}$ . The current generated can be calculated for other irradiance. The standard current, temperature and irradiance from the datasheet are used to determine the current at different

condition.  $I_{sc} \approx I_{ph}$

After calculation, gives the equation of the PV

$$I = I_{ph} - I_0 \left[ e^{\frac{q(V+I.R_s)}{a k T}} \right] - \left( \frac{V + I.R_s}{R_p} \right) \quad (3.5)$$

Where

□ diode quality factor between 1 and 2 and must be estimated. The value of “a” is equal to 1 for ideal diode.

$V$  is the cell voltage. For a PV module, the cell voltage is multiplied by the total amount of the cells found within the series.

The value of resistance series  $R_s$  is quantified from the slope  $dV/dI$  of the I-V curve at the point open circuit voltage. The equation  $R_s$  is given by

$$R_s = -\frac{dv}{di} - \frac{\frac{akT}{q}}{I_0 \cdot e^{\left(\frac{qV_{oc}}{akT}\right)}} \quad (3.6)$$

### 3.2.3 Model of the Photovoltaic module

The following model uses different method to calculate the resistance series and resistance parallel. For example, the BP MSX 120 is made of 72 solar cells (silicon nitride multi crystalline) in series and provides 120W of nominal maximum power. The maximum power point's voltage is 33.7 V and current delivered at maximum power point is 3.56 A [12]. The parameters of the BP MSX120 are given in table 3.1, which is essential to model the PV array.

TABLE 3.1

PV MODULE BP MSX120 DATASHEET AT STC

Short circuit current $I_{sc}$	3.87A
Open circuit voltage $V_{oc}$	42.1V
Current at maximum power point $I_{MPP}$	3.56A
Voltage at maximum power point $V_{MPP}$	33.7V
Number of cells in series $N_s$	72
Temperature coefficient of $I_{sc}$	(0.065±0.015)% °C
Temperature coefficient of $V_{oc}$	-(80±10)mV/°C
$P_{max}$	120W

The model consists of finding the curve characteristic of the PV module from the datasheet. The equation used to calculate the I-V curve is:

$$I = I_{ph} - I_0 \left[ e^{\frac{q(V+I \cdot R_s)}{N_s k T_a}} - 1 \right] - \left( \frac{V + I \cdot R_s}{R_p} \right) \quad (3.7)$$

The circuit model of the PV module is shown in Fig. 3.10. It is a controlled current source with the equivalent resistors and the equation of the model above. The variation of the power being taken by the load varies the PV voltage.

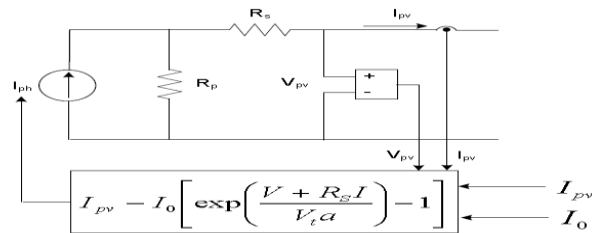


Fig. 3.10: Circuit model of the photovoltaic module

### 3.2.4 Photovoltaic array

The PV array is composed of several interconnected photovoltaic modules. The modeling process is the same as the PV module from the PV cells. The same parameters from the datasheet are used. To obtain the required power, voltage and current, the PV modules are associated in series and parallel. The number of modules connected in series and connected in parallel must be calculated. Fig. 3.11 shows a photovoltaic array, which consists of multiple modules, linked in parallel and series.  $N_{ser}$  is the total quantity of modules within the series and  $N_{par}$  is amount of modules in parallel [12]. The number of modules modifies the value of resistance in parallel and resistance in series. The value of equivalent resistance series and resistance parallel of the PV array are:

$$R_{s, \text{ array}} = \frac{R_{s, \text{ module}} \cdot N_{ser}}{N_{par}} \quad (3.8)$$

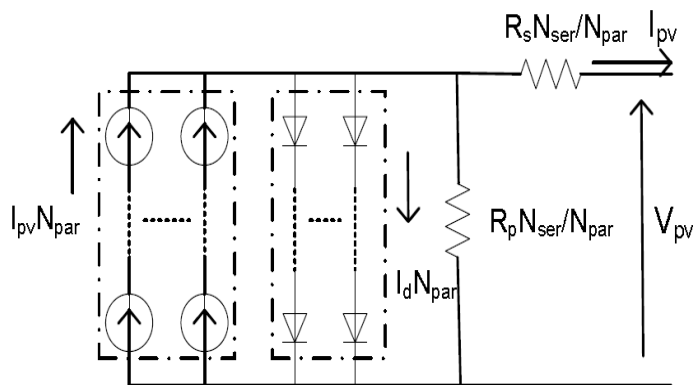


Fig. 3.11 PV Array composed of  $N_{ser} \times N_{par}$  modules

After extending the relation current voltage of the PV modules to a PV array, the new relation of current voltage of the PV array is calculated by

$$I = I_{pp}N_{par} - I_0 N_{par} \left[ \exp \left( \frac{V + R_s \left( \frac{N_{ser}}{N_{par}} \right) I}{V_t \alpha N_{ser}} \right) - 1 \right] - \frac{V + R_s \left( \frac{N_{ser}}{N_{par}} \right) I}{R_p \left( \frac{N_{ser}}{N_{par}} \right)} \quad (3.9)$$

Where  $I_0$ ,  $I_{pv}$ ,  $V_t$  are the same parameters used for a PV modules.

This equation is valid for any given array formed with identical modules.

The photovoltaic array will be simulated with this equation. The simulation circuit must include the number modules series and parallel. Fig. 3.12 shows the circuit model of the PV array.

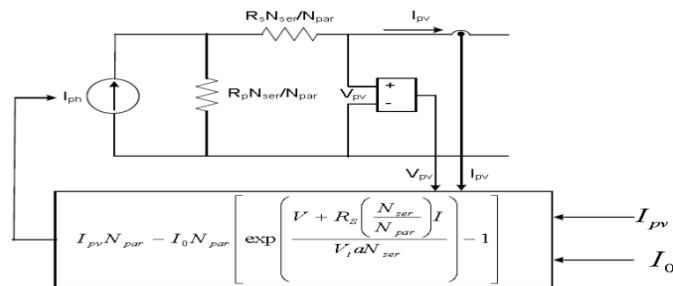


Fig. 3.12: Model structure of the photovoltaic array

### 3.3 DC/DC converter

#### 3.3.1 Operation of the boost converter

The main purpose of the DC/DC is to convert the DC input from the PV into a higher DC output. The maximum power point tracker uses the DC/DC converter to adjust the PV voltage at the maximum power point. The boost topology is used for stepping up the low voltage input from the PV. A boost type converter steps up the PV voltage to high voltage necessary for the inverter.

Fig. 3.13 shows the Boost converter. The DC input voltage is in series with an inductor L that acts as a current source. A switch T is in parallel with the current source that turns on and off periodically, providing energy from the inductor and the source to increase the average output voltage.

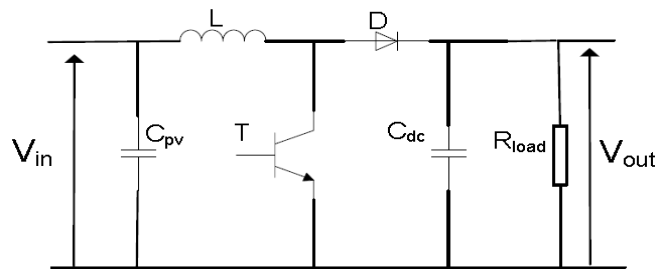


Fig. 3.13: Topology of Boost converter

The voltage ratio for a boost converter is derived based on the time integral of the inductor voltage equal to zero over switching period. The voltage ratio is equivalent to the ratio of the switching period to the off time of the switch.

$$\frac{V_o}{V_{in}} = \frac{T}{toff} = \frac{1}{1 - D} \quad (3.10)$$

The capacitor  $C_{dc}$  is large enough to keep a constant output voltage, and the inductor provides energy when the switch is open, boosting the voltage across the load.

The duty cycle from the MPPT controller is to control the switch of the boost converter. It is a gate signal to turn on and off the switches by pulse width modulation. Fig. 3.14 shows the DC/DC boost converter with the ideal switches open.

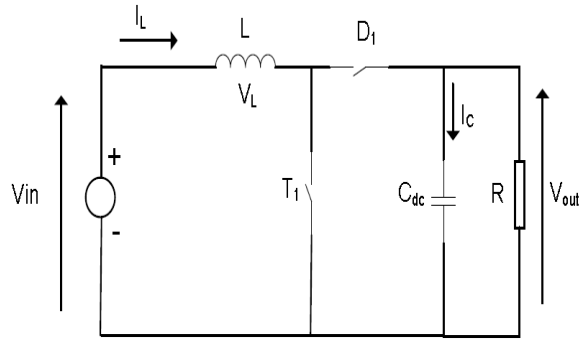


Fig. 3.14: Schematic diagram of Boost converter

In Fig. 3.15, the switch  $T_1$  is on and  $D_1$  is off, the circuit is split into two different parts: the source charges the inductor on the left while the right has the capacitor, which is responsible for sustaining outgoing voltage via energy, stored previously. The current of inductor  $L$  is increased gradually.

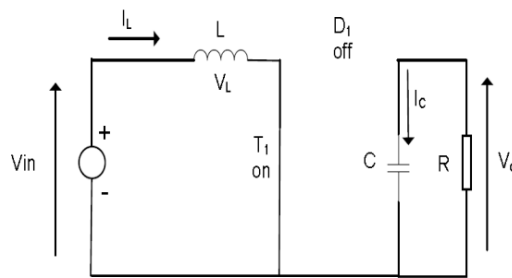


Fig. 3.15: Diagram when switch  $T_1$  is on and  $D_1$  is off

In Fig. 3.16, the switch  $T_1$  is off and  $D_1$  is on, the energy along with the DC source that is stored within the inductor will help supplement power for the circuit that is on the right thereby resulting in a boost for the output voltage. Then, the inductor current discharges and reduces gradually. The output voltage could be sustained at a particular wanted level if the switching sequence is controlled.

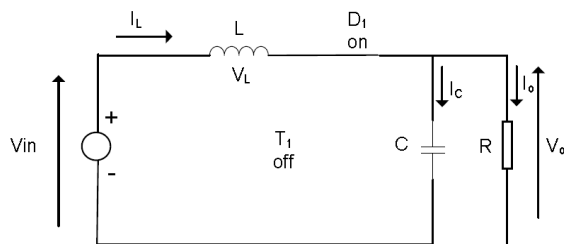


Fig. 3.16: Diagram when switch  $T_1$  is off and  $D_1$  is on



When switch  $T_1$  is turn on,  $V_L$  can be expressed as described in

$$v_L = V_{in}$$

$$i_c = \frac{-v_{out}}{R}$$

$$v_L = V_{in} - v_{out}$$

$$i_c = i_L - \frac{-v_{out}}{R} \tag{3.11}$$

While switch  $T_1$  off,  $D_1$  on

Assuming a small ripple approximation  $v_o \approx V_o$  and  $i_L \approx I$

In a stabilized condition, the time integral of the integral voltage around the course of a particular time has to be zero  $\int_0^{T_s} v_L(t) dt = (V_{in}) DT_s + (V_{in} - V_o) D' T_s$

After equating to zero, the voltage output will be:  $V_{out} = \frac{V_{in}}{D'} = \frac{V_{in}}{1-D}$

Assuming a lossless circuit  $P_{in} = P_{out}$

$$\frac{I_{out}}{I_{in}} = (1 - D) \tag{3.12}$$

It can be seen that the output voltage increases as  $D$  increases. The ideal boost converter is capable of producing any output voltage greater than the input voltage.

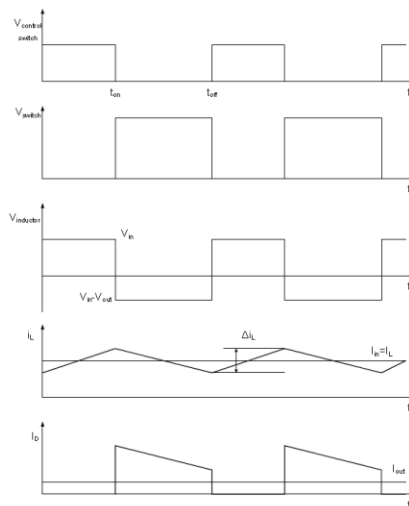


Fig. 3.17 Output waveform of DC/DC converter

### 3.3.2 Selection of the inductor

The input inductor values can be calculated based on the energy discharged during  $t_{on}$  and  $t_{off}$  times and the current ripples. In photovoltaic system, the boost converter functions in the discontinuous and continuous modes of conduction. The conduction mode of the converter could change depending on the atmospheric conditions [13]. The inductor is then calculated based on the maximum inductor current and at maximum input power. The inductor of the

$$\text{boost converter is given by } L \geq \frac{V_{om} D_m (1 - D_m)}{(f_s |\Delta I_{(L\text{ripple})}|)}$$

### 3.3.3 Power decoupling capacitor

The power decoupling capacitor  $C_{pv}$  is the capacitor linked in parallel with the PV array. It is the capacitor at the input of the boost converter. The decoupling capacitor is calculated with

$$C_{pv} \geq \frac{I_{om} \cdot D_m^2}{0.02 (1 - D_m) f_s V_{PV_{mpp}}}$$

The capacitor in parallel with the load is the DC link capacitor. The value of the capacitor depends on the minimum ripple voltage.

$$C_{DC} \geq \frac{V_{load} \cdot D}{f_s \Delta V_{Load} R_{Load}}$$

The output voltage of the PV array depends on the variation of temperature and insolation. To compensate the variation of the output voltage of the PV, a dc link capacitor is installed between the PV and the inverter. It helps to reduce the voltage ripple and provides energy storage for a short period and for a rapid change of the PV voltage

### 3.4 Six step inverter

The six-step inverter is used to obtain a three-phase voltage output from DC source. Three-phase voltage source inverter is a combination of three single-phase bridge circuits. A simplified diagram of a basic three-phase inverter bridge is shown in Fig. 3.28. There are diodes in antiparallel in addition to the main power devices.

These diodes are called the return current or feedback diodes. It provides an alternate path for the inductive current. The magnitude of the harmonic depends of the angle  $\alpha$ . Fig. 3.27 shows an example of voltage output harmonic spectrum when  $\alpha$  is 10.

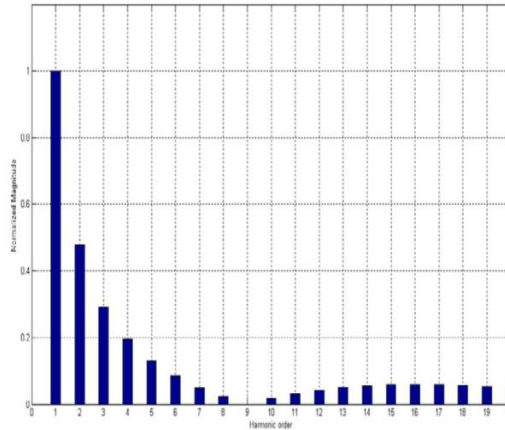


Fig. 3.18 Harmonic of output voltage when  $\alpha$  is 10.

The PWM techniques provide control scheme to reduce harmonics. The techniques can reduce the number of filter in high frequencies.

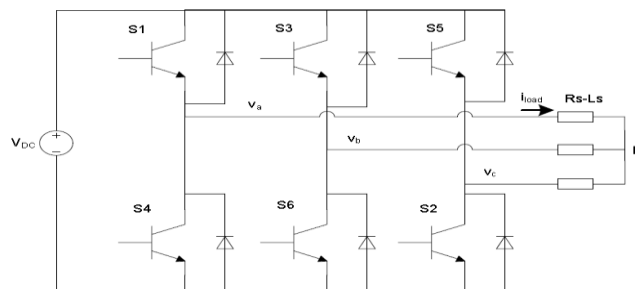


Fig. 3.19 Three-phase six-step inverter

To obtain the three-phase AC current in six-step inverter, six gating signals need to be applied to the six switches of the inverter. The waveforms of gating signals  $H_1$ ,  $H_3$  and  $H_5$  are shown in Fig. 3.29.  $H_1$ ,  $H_3$ ,  $H_5$  are 3 phase symmetrical switching function with phase shift  $120^\circ$ . To produce the symmetrical three phase voltages across a three phase load the devices are switched ON for  $180^\circ$ . The switching signals of each inverter leg are displaced by  $120^\circ$  with respect to the adjacent legs. The switching signals  $S_1$  and  $S_4$  are complimentary, the same for  $S_3$  and  $S_6$ ,  $S_5$  and  $S_2$ . The switching sequence will be  $S_1S_2S_3$ ,  $S_2S_3S_4$ ,  $S_3S_4S_5$ ,  $S_4S_5S_6$ ,

$S_5S_6S_1, S_6S_1S_2, S_1S_2S_3, \dots$  for a positive sequence. The sequence will be reversed to get the negative phase sequence.

The line to neutral voltages  $V_{an}$  represented the six step of the inverter.  $V_{bn}$  and  $V_{cn}$  have the same waveform with phase shift  $120^\circ$ .

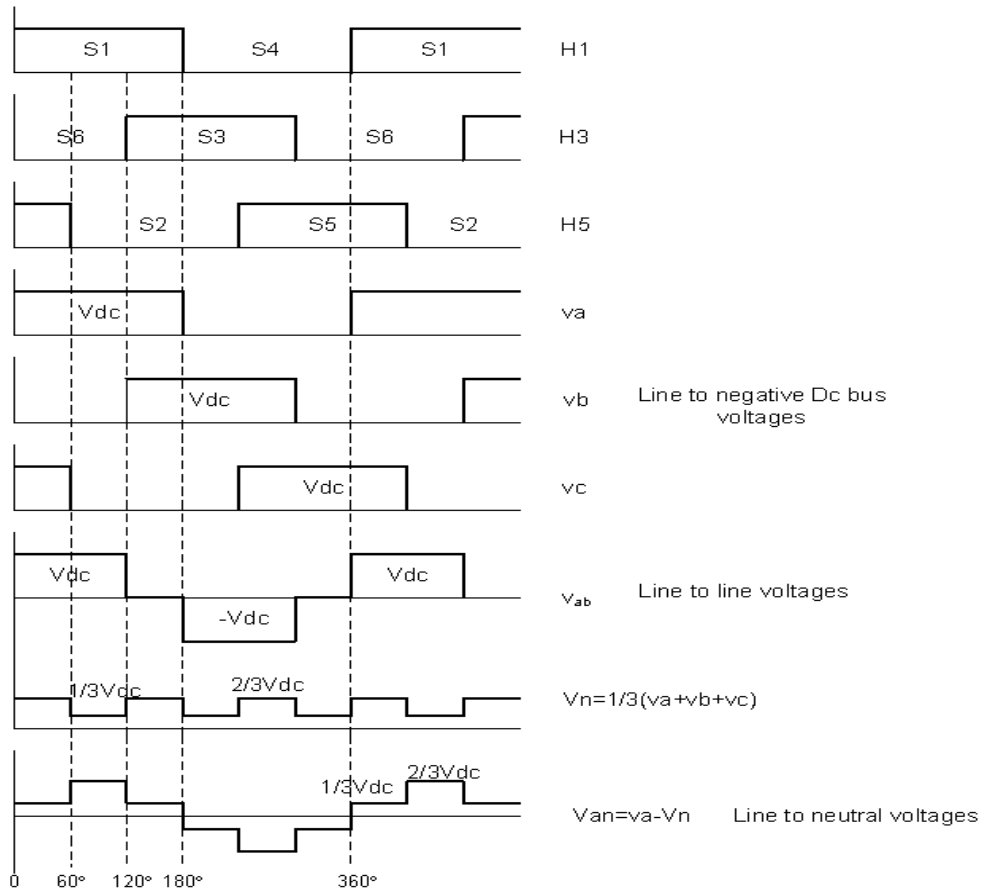


Fig. 3.20 Waveforms of the switching functions.

Each switch is turned ON for  $180^\circ$ . The switches  $S_1$  and  $S_4$ , which belong to the leftmost inverter leg, produce the output voltage for phase A. The switching signals for the switches in the middle leg,  $S_3$  and  $S_6$  for phase B, and are delayed by  $120^\circ$  from those for  $S_1$  and  $S_4$  respectively for a positive sequence. Similarly, for the same phase sequence, the switching signals for switches  $S_5$  and  $S_2$  are delayed from the switching signals for  $S_3$  and  $S_6$  by  $120^\circ$ .

It is called “six-step inverter” since there are six “steps” in the line to neutral (phase) voltage waveform as shown in Fig. 3.29.

For a six steps inverter, the outputs currents do not have harmonics of order three and multiples of three. Fig. 3.30 represents the harmonics currents of the six steps inverter.

Control over output left in a three-phase inverter could be attained by altering the voltage of the DC-link ( $V_{dc}$ )

$$(V_{an})_{1,peak} = 1.278V_{DC}/2$$

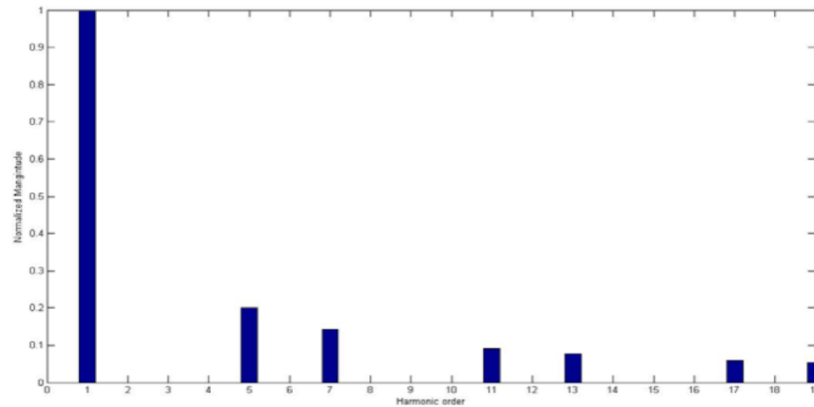


Fig. 3.21 Phase voltage normalized spectrum

In grid connected PV, the current output of the voltage source inverter will be injected to the grid. The output of the inverter should be in phase and have an identical frequency to the voltage of the grid.

### 3.5 Modulation strategies

#### 3.5.1 SVPWM techniques

The three-phase power inverter is the same represented in Fig. 3.28. There are six power switches  $S_1$  to  $S_6$ . Each of them is controlled by individual switching variables which are obtained from the principles of space vector PWM.

The three-phase voltage in abc reference frame should be represented in dq reference frame for the Space vector PWM. The output voltages can be represented in the space as set of vectors. These vectors correspond to switching combinations for the inverter switches. There are eight combinations for the voltage output as is made evident in Fig. 3.31. The three phase output voltages in the full bridge inverter at any instant of time can be represented by a set of

eight base space vectors as per the eight positions of switching in terms of the inverter [13]. The principle of Space vector PWM is one cycle of the output voltage that can be represented by six sectors ( $60^\circ$  each). A rotating reference voltage  $V_{ref}$  that is calculated through an estimate based on 3 adjacent vectors represent the desired output voltage.

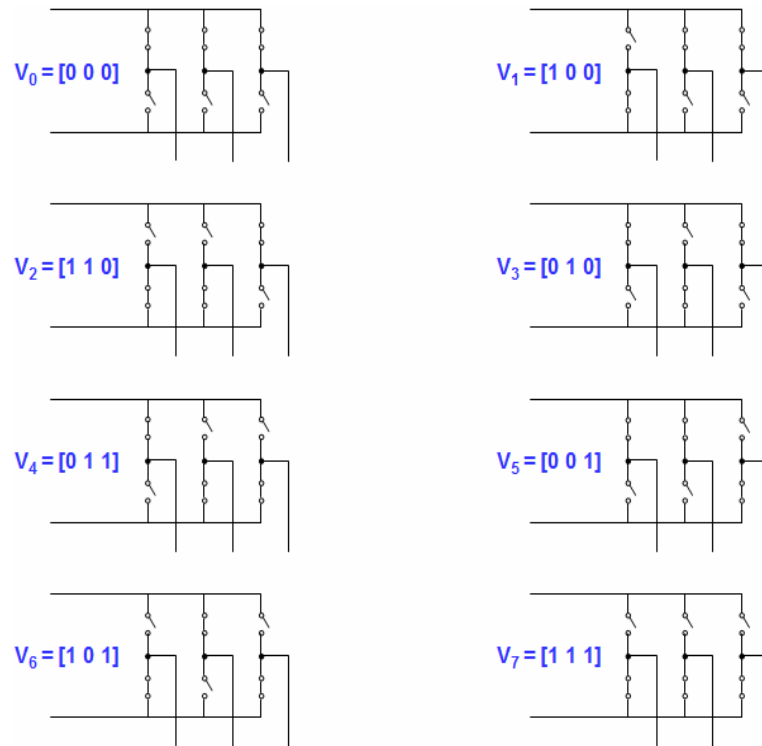


Fig. 3.22 Eight switching states

Fig. 3.32 shows these base vectors  $V_1$  through  $V_6$  and the two zero vectors  $V_0$  and  $V_7$  which correspond to switching positions resulting in zero output voltage.

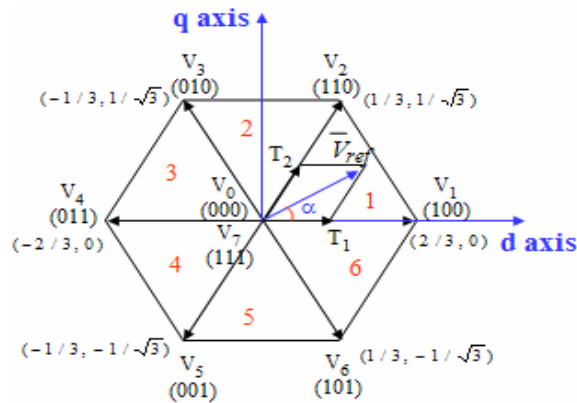


Fig. 3.23 Switching vectors and the 6 sectors

Fig. 3.32 shows the approximate reference voltage vector  $V_{ref}$ , which uses the eight switching patterns ( $V_0$  to  $V_7$ ). In space vector modulation, the voltage vectors  $V_0$  to  $V_7$  for certain instances are applied in a manner that the “mean vector” of the PWM period  $T_z$  is equal to the desired voltage vector.

The principle of space vector PWM technique is that the voltage vector command is calculated by estimation via three adjacent vectors base. It is necessary to decompose the space voltage vector into directions of the sector base vectors. For instance, if  $V_{ref}$  is located in sector 1(Fig. 3.32), the base vectors are  $V_1$ ,  $V_2$  and  $V_0$  ( $V_7$  can also be used because it gives the same output voltage), if  $V_{ref}$  is located in sectors 2, the base vector surrounding  $V_{ref}$  are  $V_2$ ,  $V_3$  and  $V_0$ . The time span of every vector for the voltage is taken by calculations in sector 1 where

$$T_z V_{ref} = T_1 V_1 + T_2 V_2 + T_0 V_0 \quad (3.13)$$

$T_z = T_1 + T_2 + T_0$  Where  $V_1$ ,  $V_2$  and  $V_0$  basically outline the triangular area in which  $V_{ref}$  are found.  $T_1$ ,  $T_2$  and  $T_0$  are the matching vector periods and  $T_z$  is the sampling time

$V_1$  (100) is applied for a period of  $T_1$

$V_2$  (110) is applied for period  $T_2$

$V_0$  (000) or  $V_7$  (111) is applied for period of  $T_0$  for this sector.

TABLE 3.2

SWITCHING STATES OF THE INVERTER SWITCHES

Voltage Vectors	Switching Vectors			Line to neutral voltage $\times V_{dc}$			Line to line voltage $\times V_{dc}$		
	a	b	c	$V_{an}$	$V_{bn}$	$V_{cn}$	$V_{ab}$	$V_{bc}$	$V_{ca}$
$V_0$	0	0	0	0	0	0	0	0	0
$V_1$	1	0	0	$2/3$	$-1/3$	$-1/3$	1	0	-1
$V_2$	1	1	0	$1/3$	$1/3$	$-2/3$	0	1	-1
$V_3$	0	1	0	$-1/3$	$2/3$	$-1/3$	-1	1	0
$V_4$	0	1	1	$-2/3$	$1/3$	$1/3$	-1	0	1
$V_5$	0	0	1	$-1/3$	$-1/3$	$2/3$	0	-1	1
$V_6$	1	0	1	$1/3$	$-2/3$	$1/3$	1	-1	0
$V_7$	1	1	1	0	0	0	0	0	0

Determination of time duration T1, T2, T0

$$T_z \cdot V_{ref} \cdot \begin{bmatrix} \cos \alpha \\ \sin \alpha \end{bmatrix} = T_1 \cdot \frac{2}{3} V_{dc} \begin{bmatrix} 1 \\ 0 \end{bmatrix} + T_2 \cdot \frac{2}{3} V_{dc} \begin{bmatrix} \cos \pi/3 \\ \sin \pi/3 \end{bmatrix}$$

$$0 \leq \alpha \leq \pi/3 \text{ and define } a = \frac{|V_{ref[\alpha,\beta]}|}{\frac{2}{3}V_{dc}}$$

$$T_1 = T_z \cdot a \cdot \frac{(\sin \pi/3 - \alpha)}{\sin \pi/3}$$

$$T_2 = T_z \cdot a \cdot \frac{\sin \alpha}{\sin \pi/3}$$

$$T_0 = T_z - T_2 - T_1 \tag{3.14}$$

Switching time duration at any sector

The base vectors change for each sector. Let define n is the sector 1 to 6 and  $0 \leq \alpha \leq 60^\circ$

$$T_1 = \frac{\sqrt{3} \cdot T_z \cdot |V_{ref}|}{V_{dc}} \left( \sin \left( \frac{\pi}{3} - \alpha + \frac{n-1}{3}\pi \right) \right)$$

$$T_1 = \frac{\sqrt{3} \cdot T_z \cdot |V_{ref}|}{V_{dc}} \left( \sin \frac{n}{3}\pi \cos \alpha - \cos \frac{n}{3}\pi \sin \alpha \right)$$

$$T_2 = \frac{\sqrt{3} \cdot T_z \cdot |V_{ref}|}{V_{dc}} \left( \sin \left( \alpha - \frac{n-1}{3}\pi \right) \right)$$

$$T_2 = \frac{\sqrt{3} \cdot T_z \cdot |V_{ref}|}{V_{dc}} \left( \sin \alpha \cdot \cos \frac{n-1}{3}\pi - \cos \alpha \cdot \sin \frac{n-1}{3}\pi \right)$$

$$T_0 = T_z - T_1 - T_2 \tag{3.15}$$

The duration T1, T2 and T0 are applied for each sector to calculate the output voltage. The switching pattern is determined to have less switching of the devices. For instance in sector 1, Tz can be decomposed as

$$T_z = \frac{T_0}{4} \cdot V_0 + \frac{T_1}{2} \cdot V_1 + \frac{T_2}{2} \cdot V_2 + \frac{T_0}{4} \cdot V_7 + \frac{T_0}{4} \cdot V_7 + \frac{T_2}{2} \cdot V_2 + \frac{T_1}{2} \cdot V_1 + \frac{T_0}{4} \cdot V_0 \tag{3.16}$$

This arrangement allows preventing un-necessary switching and lowering switching losses in practice and always maintains the total duration period Tz. Such arrangement is used for all



the 6 sectors. It allows having the voltage  $V_0$  at the start and end of every cycle so when  $T_z$  repeats; there is no need to change the states of the switches.

In sector 2, the base voltages are  $V_2$  and  $V_3$ ; for sector 3, the base voltages are  $V_3$  and  $V_4$ . Sometimes the order of  $T_1$  and  $T_2$  can be interchanged to avoid the change of the state of the switches and to minimize the switching losses. If the switching frequency is 5400 Hz then  $1/T_z = 5400 \text{ Hz}$  and the fundamental frequency is 60 Hz, then  $T_z$  repeats 15 times for each sector. For one period, the output voltage can be represented by 90 vectors. The switching time and switching sequence at each sector is summarized in Fig. 3.33. In this situation, the switching waveforms are symmetrical [14]. The switching sequence is described below each switching pattern, for example for sector 1, switching sequence is 0,1,2,7,7,2,1,0, for sector 2, switching sequence is 0,3,2,7,7,2,3... and so on.

The DC input of the SVPWM is the output from the boost converter.

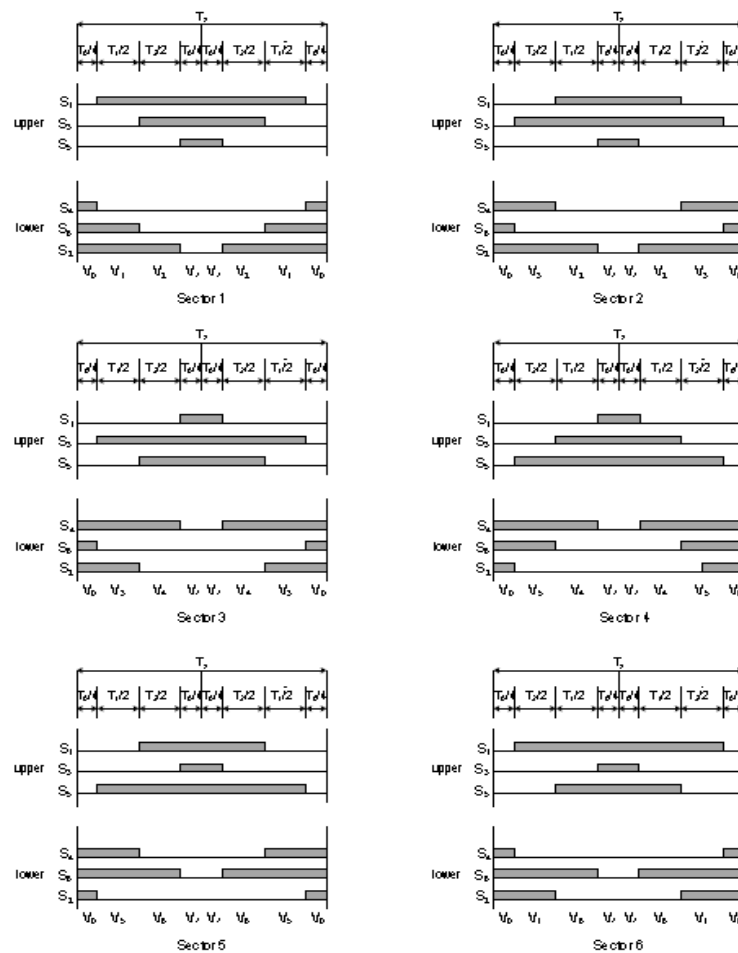


Fig. 3.24 Space vector PWM switching patterns and sector duration

### 3.5.2 Sine PWM

In sine-triangle three-phase PWM inverter, three sinusoidal reference voltage waveforms at each phase are compared to the same triangular carrier. The three-reference voltages are 120° apart.

$$v_{a,ref} = V_{ref} \sin(2\pi f \times t)$$

$$v_{b,ref} = V_{ref} \sin(2\pi f \times t - 2\pi/3)$$

$$v_{c,ref} = V_{ref} \sin(2\pi f \times t + 2\pi/3)$$

(3.17)

With this method, switch  $S_1$  is ON when triangular carrier is less than and  $S_4$  is OFF. The output voltage is equal to  $V_{dc}$ . The same principles apply for the other legs of the converter. To summarize the principles:

$$v_{a,ref} > V_{tria} \rightarrow S1 \text{ is ON}$$

$$v_{a,ref} < V_{tria} \rightarrow S4 \text{ is ON}$$

$$v_{b,ref} > V_{tria} \rightarrow S2 \text{ is ON}$$

$$v_{b,ref} < V_{tria} \rightarrow S5 \text{ is ON}$$

$$v_{c,ref} > V_{tria} \rightarrow S3 \text{ is ON}$$

(3.18)

Fig. 3.34 shows the waveform of the sine triangle and the voltage reference comparison.

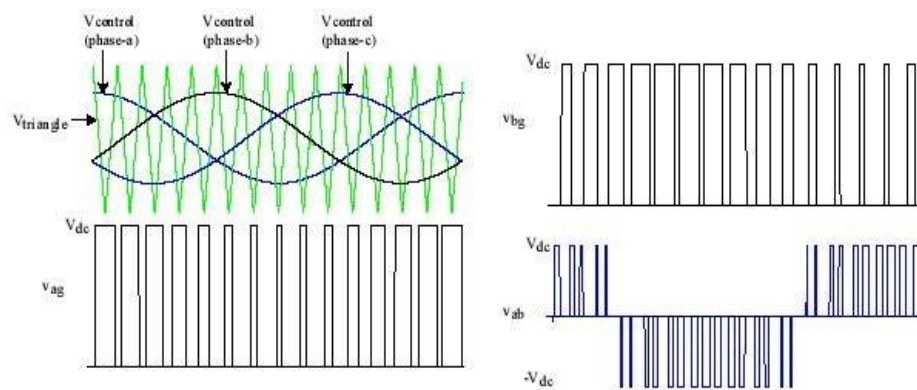


Fig. 3.25 Sine triangle, voltage reference and phase voltage

In sine triangle PWM, the amplitude modulation ratio (or index)  $m_a$  is defined by

$$m_a = \frac{\text{peak amplitude of } V_{tria}}{\text{amplitude of } V_{ref}}$$

The frequency of the triangular waveform  $f_{pwm}$  is the frequency of the inverter. The frequency of the reference is the fundamental output frequency. For a grid connected PV, it is the frequency of the grid 50 Hz. The ratio of those two frequencies gives the frequency modulation index

$$m_f = \frac{\text{PWM frequency } f_{pwm}}{\text{fundamental frequency } f_1}$$

The line to neutral fundamental frequency output voltage of the inverter is defined by

$$\begin{aligned} v_{an,1} &= \frac{m_a V_{DC}}{2} \sin(2\pi f_0 \cdot t) \\ v_{bn,1} &= \frac{m_a V_{DC}}{2} \sin(2\pi f_0 \cdot t - \frac{2\pi}{3}) \\ v_{cn,1} &= \frac{m_a V_{DC}}{2} \sin(2\pi f_0 \cdot t + \frac{2\pi}{3}) \end{aligned} \tag{3.19}$$

The line-to-line voltage rms value at the fundamental frequency is obtained by multiplying the fundamental line to neutral fundamental frequency with  $\sqrt{3}/\sqrt{2}$ .

The switching frequency should be higher to reduce the harmonics at the output. Thus, less filter harmonics will be used [15]. However, switching losses increase in proportion to the switching frequency.

In PV system, the DC voltage that is the output from the boost converter is the input for the inverter. A controller should be implemented in order to maintain the DC voltage in a constant manner. In addition, the voltage reference determines the output frequency and amplitude desired [16].

The function of inverter DC/AC is to generate AC output current  $i_{ac}$  in phase with the AC grid voltage  $v_{ac}$ . switching frequency  $f_{pwm}$  is much greater than the AC line frequency (60Hz

or 50Hz). By controlling the switch duty ratio  $D$  of the inverter, it is possible to generate a sinusoidal current  $i_{ac}$  in phase with the AC line voltage. The input DC voltage  $V_{dc}$  must be greater than the peak AC line voltage.

### 3.6 Control of the boost converter with MPPT controller

#### 3.6.1 Maximum power point techniques for PV

From the characteristic I-V and P-V curves of photovoltaic modules, it is shown that there was a unique point for the maximum power (PMPP). This point is defined as the maximum power point (MPP) with the optimal voltage  $V_{mpp}$  and the optimal current  $I_{mpp}$ . At this point, the entire PV system should operate with the maximum efficiency and produce its maximum output power.

The solar cell I-V characteristic is nonlinear and changes with irradiation and temperature. The location of the MPP is not known but need to be located. Different MPPT methods have been realized. They vary in “complexity, sensors required for the voltage or current, convergence speed, and cost, range of effectiveness and implementation hardware”.

The three main categories of MPPT algorithms are model-based algorithms, training based algorithms and searching algorithms [17].

Model-based MPPT algorithm

MPPT with Fractional short-circuit current method

This method is based on the measurement periodically of the PV short circuit current, which is approximately linear to the current maximum power point as shown in

$$I_{MPP} \approx k_2 I_{sc}$$

Experimentally,  $k_2$  is a constant between 0.78 and 0.92. Once the constant  $k_2$  is known,  $I_{MPP}$  is computed. The PV array needs to be shorted periodically to measure  $I_{sc}$ .

Fractional open circuit voltage

Similarly, the Fractional open-circuit voltage is based on the linear dependence between array voltages at maximum power  $V_{MPP}$  with its open circuit voltage  $V_{oc}$

$$V_{MPP} \approx k_1 V_{oc}$$

$k_1$  is a constant between 0.71 and 0.78.  $V_{oc}$  is measured by shortly shutting down the power converter.

The implementations of those methods are simple and cheap but here is excessive power loss and the efficiency of the PV is very low due to the inaccurate determination of the constant  $k_1$  and  $k_2$ . The power loss is caused by the necessity to open and close the circuit for measurement [18].

### 3.6.2 Perturb & Observe P&O/ Hill Climbing

P&O and Hill climbing use the same fundamental strategy. The duty ratio is the perturbation in hill climbing, while the voltage of the PV module is the perturbation for the P&O. Changing the value of the duty cycle causes a change to the current and as consequence, perturbs the voltage array. In Fig. 3.35, the voltage and current are measured and the MPPT controller determines the voltage reference. The input for the regulator PI is the difference of the  $V_{ref}$  and  $V_{pv}$ . The voltage regulated generates the PWM for the converter.

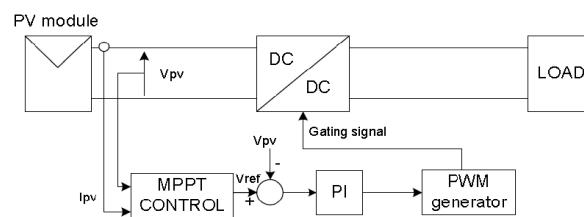


Fig. 3.26 Block diagrams of MPPT with P&O

For Hill climbing, there is no regulator, only the duty ratio controls the converter directly as shown in Fig. 3.36.

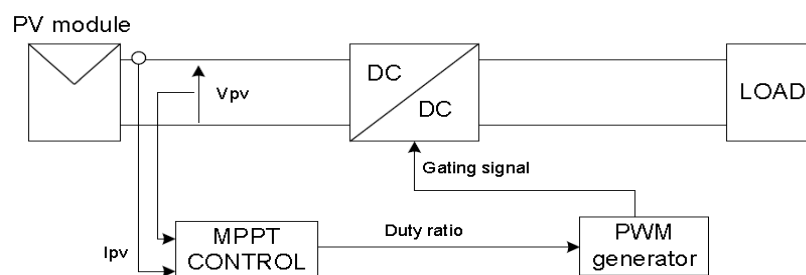


Fig. 3.27 Block diagrams of MPPT with Hill Climbing

In Fig. 3.37, it can be observed that incrementing the PV voltage increases the power of the PV and decrementing the PV voltage decreases the power of the PV when operating on the left of the MPP. On the right of MPP, incrementing the voltage decreases the power and decrementing the voltage increases the power [19]. This process will be implemented in the MPPT controller to extract the maximum power from the PV module.

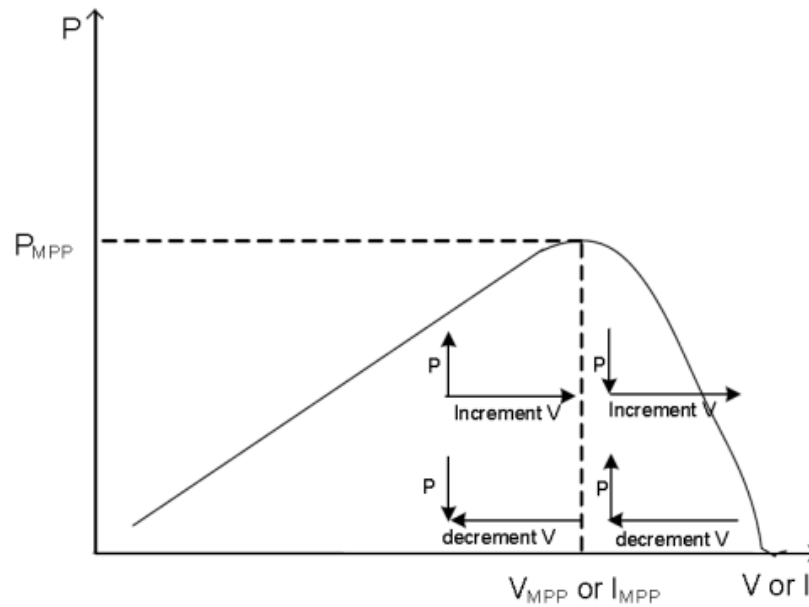


Fig. 3.28 Principle of P&O

# CHAPTER 4

## SIMULATION OF THE PHOTOVOLTAIC SYSTEM USING MATLAB / SIMULINK

### 4.1 Simulation of the photovoltaic module

The simulation of the photovoltaic module is realized with Simulink model. The simulation allows having the curve I-V and P-V characteristics.

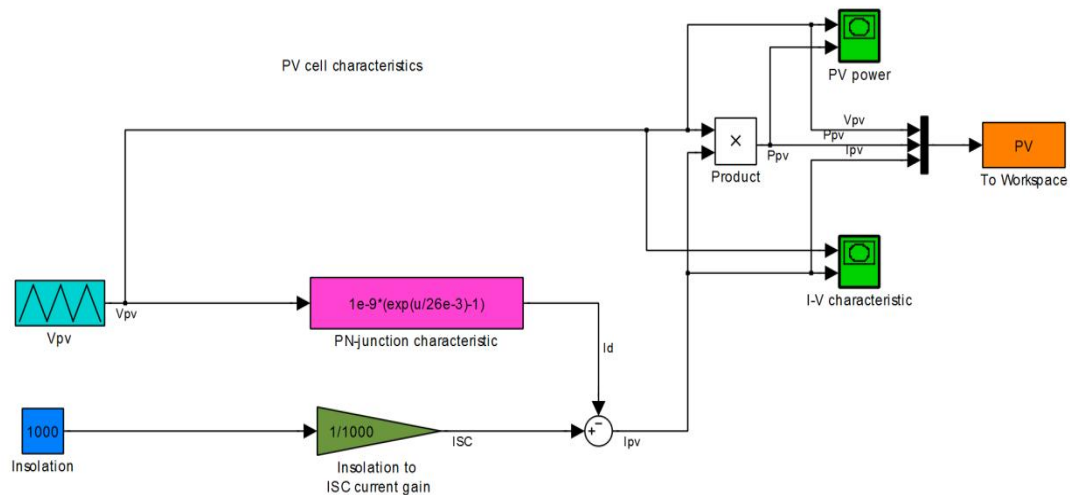


Fig. 4.1 Simulation of the PV module

Certain variables are modified for the application with maximum power point tracking. The input parameters required for the model are:

The PV characteristics from data sheet are used to generate the file necessary for  $R_s$ ,  $R_p$  and other parameters for the maximum power point [20]. The initial setup is used to obtain the I-V curve characteristics of the PV array and show the maximum power point of the PV. The model of the PV is used with the boost converter to determine the performance of the maximum power point tracker.

The model of the photovoltaic array has been implemented in Simulink as shown in Fig. 4.2. The irradiance is specified. The simulation allows having the curve I-V and P-V characteristics. The Simulink model uses a current source, voltage source and the value of the resistance in series and parallel of the PV.

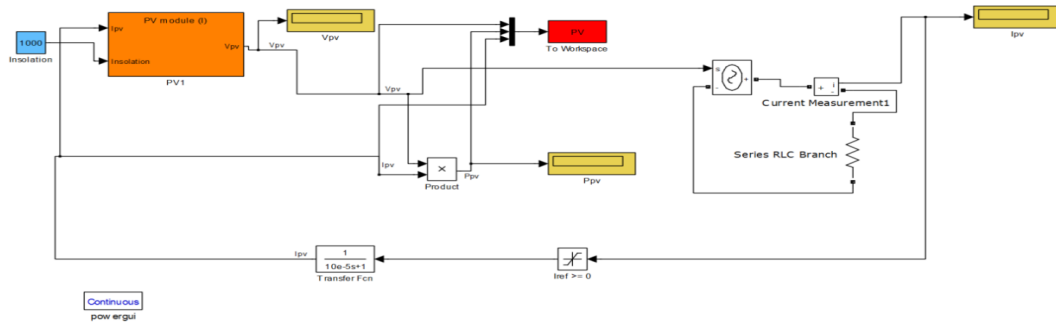


Fig. 4.2 Simulation of the PV array

The proposed system will consist of PV arrays, a step-up dc–dc converter, a grid-tie inverter (GTI) and an automatic AC transfer switch. PV arrays convert solar energy into electric energy. Step-up dc–dc converter boosts the array voltage to a higher level; the GTI inverts the DC power produced by the PV array into AC power aligned with the voltage and power quality requirements of the utility grid and the transfer switch changes supply source and also selects serving loads according to availability.

In normal condition, the system power up on-site electrical loads and serve energy to the grid if the system output is greater than the on-site demand. Net metering would allow the homeowner to sell energy back to government. But when the utility grid power is not available or when the utility voltage level or frequency goes beyond accepted limits, the system automatically disconnects the grid through an anti-islanding scheme. In this condition, existing battery less grid-tied PV systems do not serve the residential loads also. But in our proposed design it will supply residential loads during the grid failure or blackout for load shedding by an automatic AC transfer switch [21]. This feature is indispensable considering the grid load shedding condition in state

Configuration of a typical grid-tied PV system is depicted below in Fig. 4.3

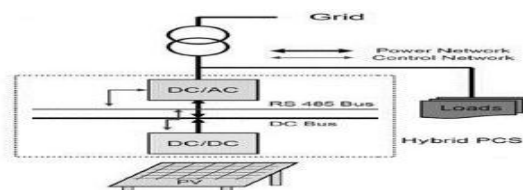


Fig. 4.3 Grid connected system

## 4.2 Simulink model of boost converter



Fig. 4.4 shows the Simulation of the boost converter. The input of the boost converter is the photovoltaic output voltage. The inductance and the capacitor need to be specified.

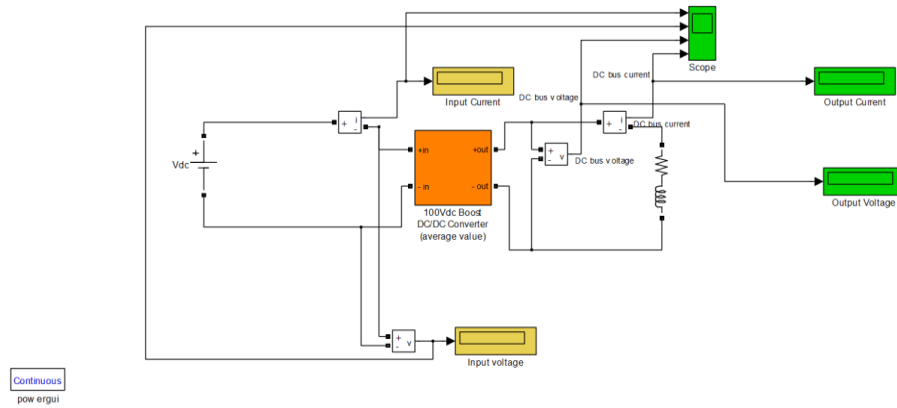


Fig. 4.4 Simulation of the DC-DC converter

The voltage and the current of the photovoltaic array are the input, and the duty cycle is the output. The duty cycle is compared to a triangle wave signal to generate the PWM. The frequency of the triangle wave is the pulsation frequency of the boost converter.

Fig. 4.5 is the simulation of the Boost converter and the photovoltaic array in Simulink. The system has a resistive load to test the simulation.

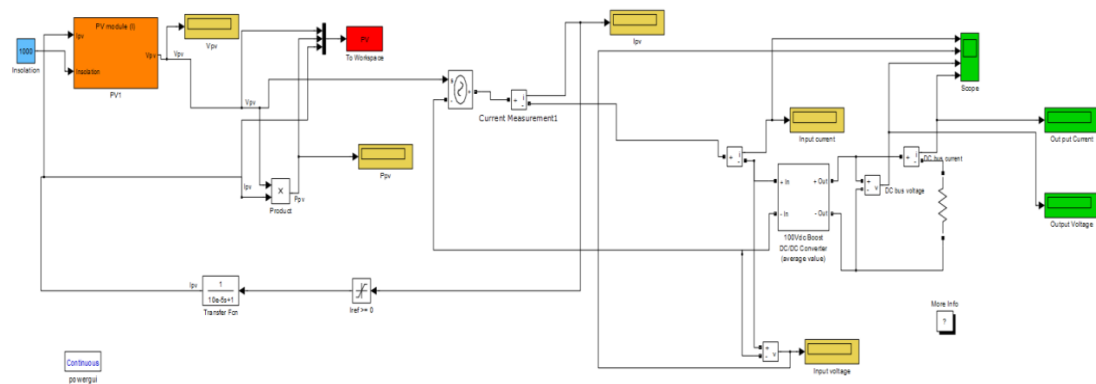


Fig. 4.5 Simulink model of the photovoltaic system with dc-dc converter

### 4.3 Simulink model of the photovoltaic system with AC-DC-AC PWM converter

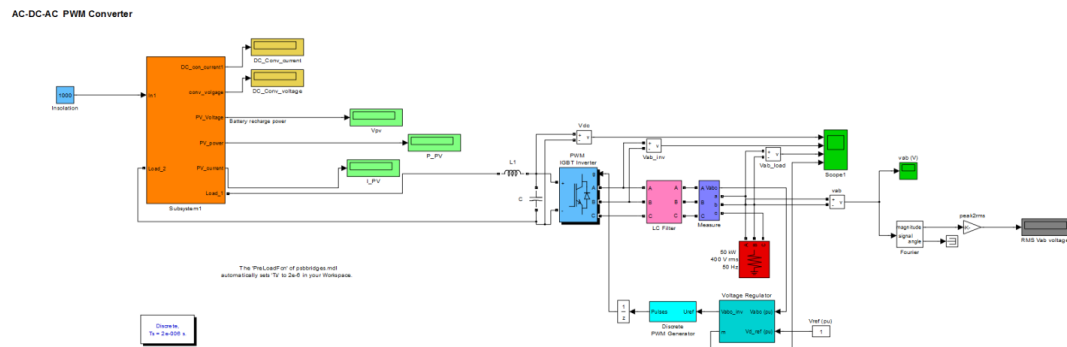


Fig. 4.6 Simulation of the PV system with boost and three-phase inverter

The PV system with three-phase inverter shown in Fig. 4.6 is used. The three-phase inverter has three-phase inductance filter and resistance load. An inverter block from Simulink is the three-phase inverter. The PV and boost, remain the same. The pulse generator produces the gating signal for the inverter block. The output voltage from the boost converter is the DC voltage for the three-phase inverter.

### 4.4 Simulink model of the photovoltaic system with MPP

The maximum power point controller block is shown in Fig. 4.8 The voltage and the current of the photovoltaic array are the input, and the duty cycle is the output.

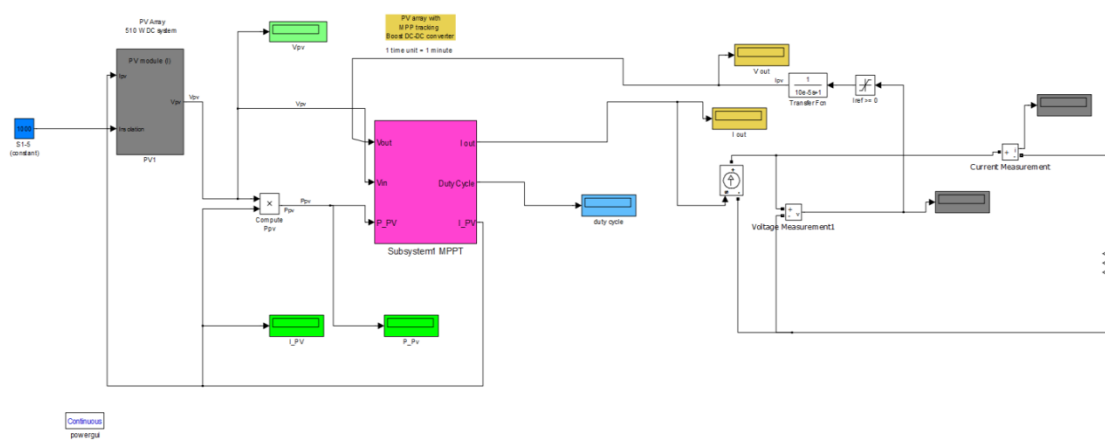


Fig. 4.7 Simulation of the PV system with MPPT

The duty cycle is compared to a triangle wave signal to generate the PWM. The frequency of the triangle wave is the pulsation frequency of the boost converter.

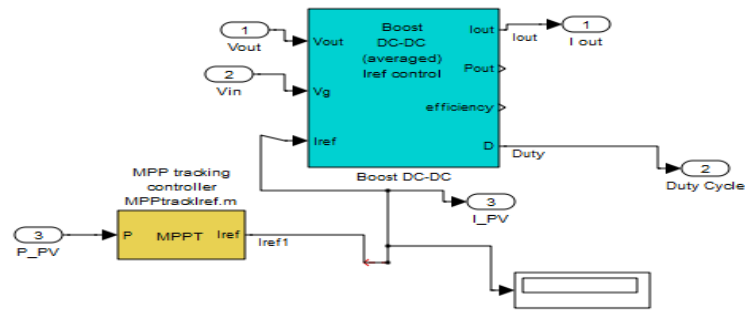


Fig. 4.8 Simulation of the DC to dc converter with MPPT

The perturb and observe algorithm is implemented and shown in Fig. 4.9. The duty cycle is increased or decreased until the maximum power point of the photovoltaic is reached. The step of the duty cycle is constant, and it determines the efficiency and accuracy of the MPPT controller.

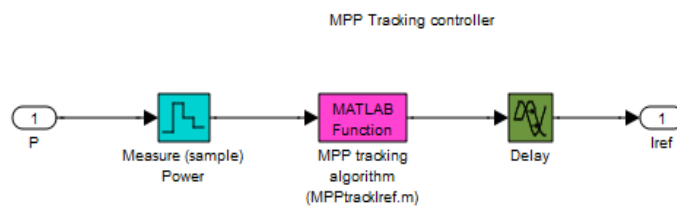


Fig. 4.9 Simulation of the perturb and observe algorithm

#### 4.5 Simulink model of the photovoltaic system with MPPT and Battery

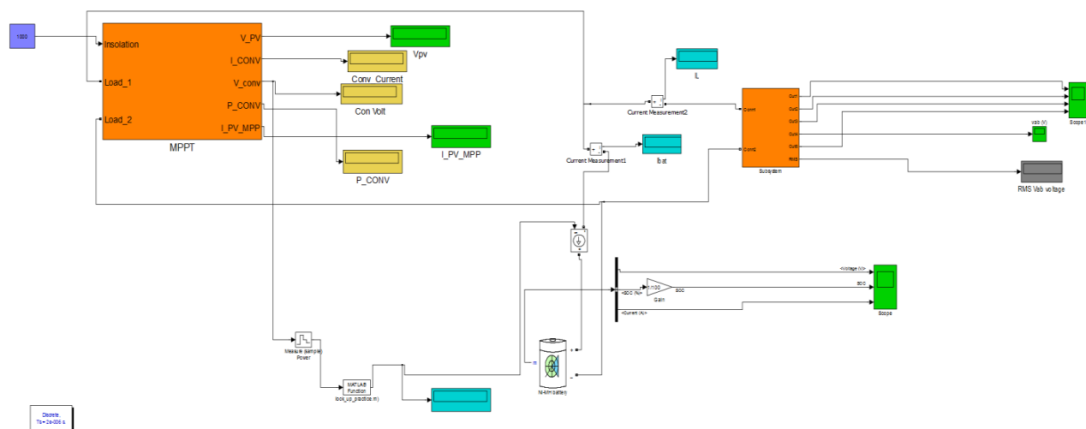


Fig. 4.10 Simulation of the PV system with MPPT and battery

The simulation of PV with MPPT and Battery is shown in Fig. 4.10 which is connected with the 50 KW load.

#### 4.6 Simulink model of Grid connected Photovoltaic system

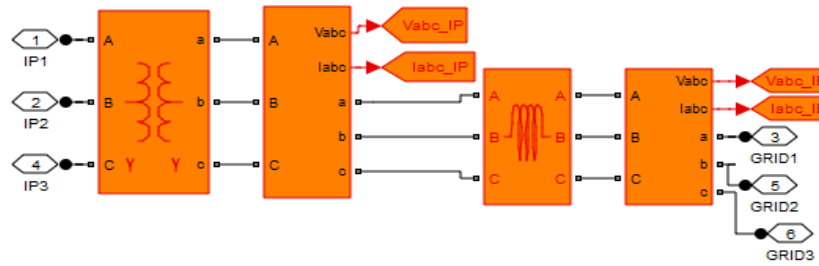


Fig. 4.11 interconnection between grid and inverter

Fig. 4.11 shows the interconnection between grid and inverter. Here transformer used for the

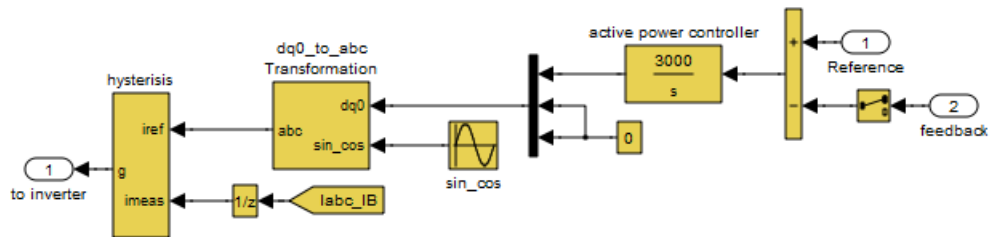


Fig. 4.12 Grid synchronizing

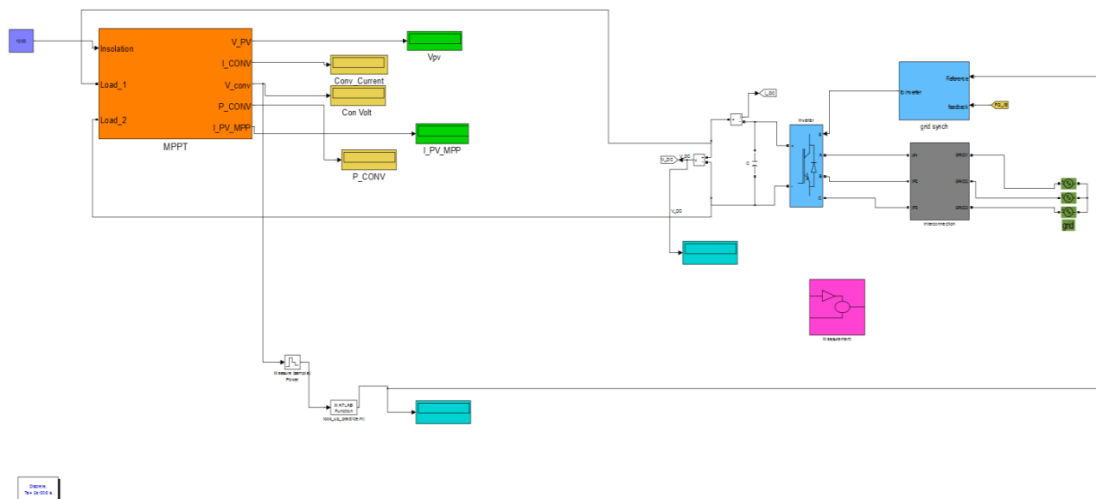


Fig. 4.13 Simulation of Grid connected Photovoltaic system

The simulation model of Grid connected Photovoltaic system is shown in Fig. 4.13. The three-phase inverter has three-phase inductance filter and resistance load. An inverter block from Simulink is the three-phase inverter [22]. The PV, boost and MPPT, remain the same. The pulse generator produces the gating signal for the inverter block. The output voltage from the boost converter is the DC voltage for the three-phase inverter.

## CHAPTER 5

# SIMULATION RESULT OF THE PHOTOVOLTAIC SYSTEM USING MATLAB / SIMULINK

### 5.1 Simulation result of photovoltaic system

The model of the photovoltaic system in the previous chapter is used to determine the performance of the MPPT controller with boost converter. This simulation presents an analysis of the photovoltaic array with boost converter and resistive load. The temperature, irradiance and load, are varied to determine the performance of the MPPT and track the maximum power of the PV. The major component of Grid-tied PV system is the GTI which along with regulating the voltage and current received from solar panels ensures that the power supply is in phase with the grid power. On AC side, it keeps the sinusoidal output synchronized to the grid frequency (nominally 50Hz). The voltage of the inverter output needs to be variable and a touch higher than the grid voltage to enable current to supply the loads in the house or even supplies excess power to the utility.

### 5.2 Photovoltaic array characteristics

#### 5.2.1 The I-V and P-V characteristics of single cell

Fig shows the I-V and P-V characteristics and table shows the maximum power point of the single cell at the different insolation.

**1000W/m<sup>2</sup>**

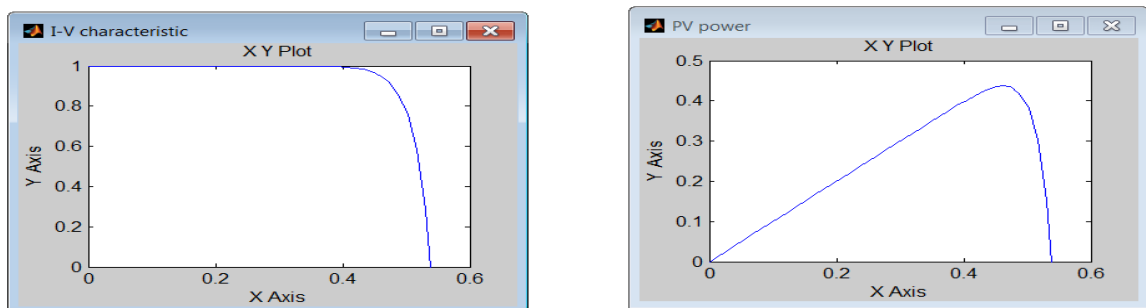


Fig. 5.1 I-V curve and P-V curve of the BP MSX 120 module

**800W/m<sup>2</sup>**

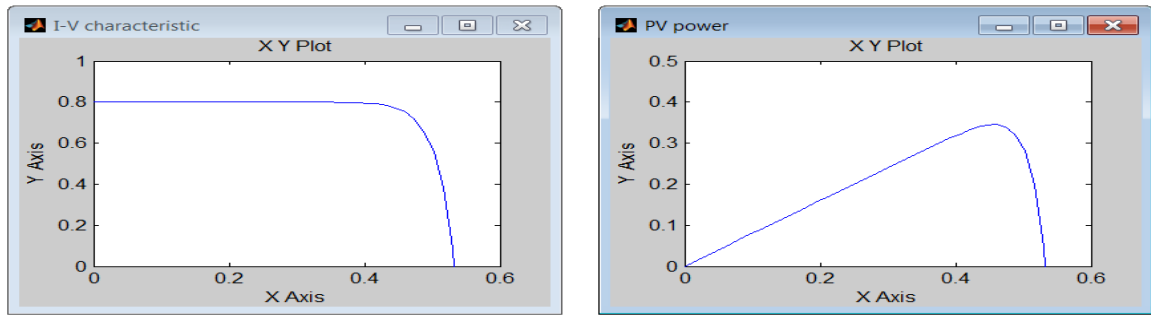


Fig. 5.2 I-V curve and P-V curve of the BP MSX 120 module

**600W/m<sup>2</sup>**

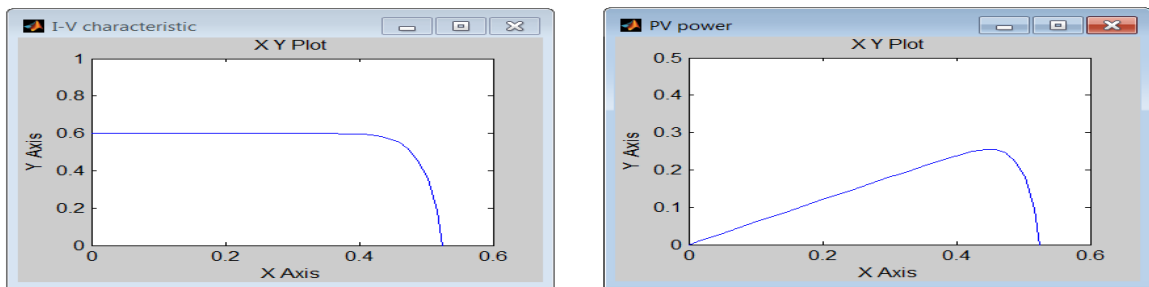


Fig. 5.3 I-V curve and P-V curve of the BP MSX 120 module

TABLE 5.1

PHOTOVOLTAIC MODULE MAXIMUM POWER POINT VALUES AT 1000, 800 & 600W/M<sup>2</sup>

<b>Rating</b>	<b>MPP power</b>	<b>MPP Voltage</b>	<b>MPP Current</b>
1000W/m <sup>2</sup>	0.4378	0.46	0.9517
800W/m <sup>2</sup>	0.3458	0.46	0.7517
600W/m <sup>2</sup>	0.255	0.446	0.5718

The photovoltaic model used is the NE-80EJEA. It has a maximum power output 80 W. The table 5.2 gives the characteristic of the module NE-80EJEA at STC 25C.

TABLE 5.2

## PV MODULE NE-80EJEA DATA SHEET VALUES AT STC

Short circuit current $I_{SC}$	5.45 A
Current at maximum power point $I_{MPP}$	4.95 A
Voltage at maximum power point $V_{MPP}$	17.6 V
Open circuit voltage $V_{OC}$	22.2 V
Number cells in series $n_s$	36

The module NE-80EJEA is connected in series and parallel to achieve a maximum power output of 26 kW and output voltage 753 V. Table 5.3.gives the characteristic of the PV for maximum power 26 kW. A PV of 26 KW is made from the NE-80EJEA with 25 modules in series and 10 modules in parallel. The current and voltage at maximum power are respectively 64.49 A and 753 V.

TABLE 5.3

## CHARACTERISTICS OF 26 KW PHOTOVOLTAIC

Number of modules in a string series $N_{SS}$	25
Number of modules in a string parallel $N_{PP}$	10
Output voltage rating	753 V
Output current rating	64.49 A
Maximum power output	26000W

**5.3 Photovoltaic system with a Boost converter**

The simulation presents an analysis of the photovoltaic array 26000W with the boost converter.



The PV system parameters are:

**DC bus voltage  $V_{dc}$ : 400 V**

The boost parameters are calculated and the inductance and capacitance values are given below. The boost input voltage nominal is 400 V and, the output voltage is 500 V

### 5.3.1 R-L type load

TABLE 5.4

$$R = 100 \times 100 / 6000 = 1.666 \, \Omega, \quad L = 100 \times 100 / 6000 = 1.666 \, \text{H}$$

Input	Output
$V_{dc} = 400$	$V_{dc} = 500$
$I_{dc} = 372.5$	$I_{dc} = 298$

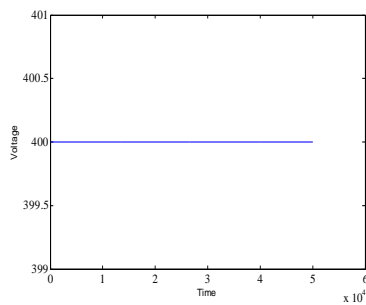
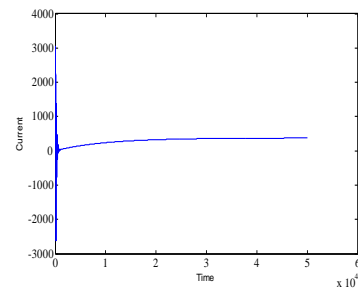


Fig. 5.4 (a) DC I/P Voltage



(b) DC I/P Current

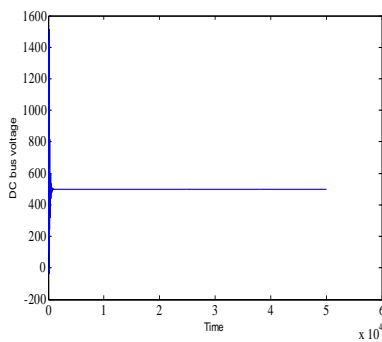
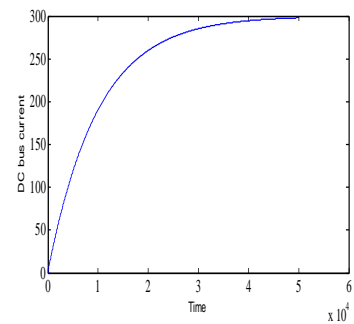


Fig. 5.5 (a) DC Bus Voltage



(b) DC Bus Current

### 5.3.2 Change input voltage waveform of DC-DC converter with 400 V constant

TABLE 5.5

#### INPUT /OUTPUT

Input	Output
$V_{dc} = 450$	$V_{dc} = 500$

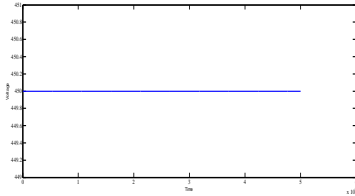
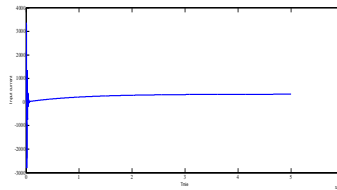


Fig. 5.6 (a) Input Voltage



(b) Input Current

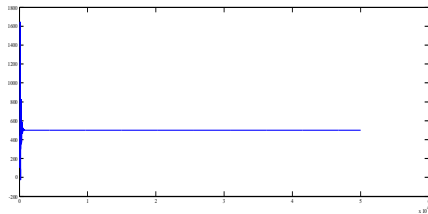
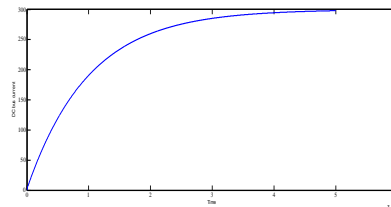


Fig.5.7 (a) DC Bus Voltage



(b) DC Bus Current

### 5.3.3 DC-DC converter

Above both the waveform we show that when we change the input voltage there is no effect on output.

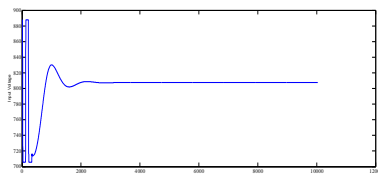
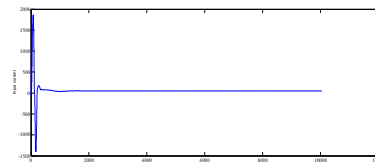


Fig 5.8 (a) Input Voltage



(b) Input Current

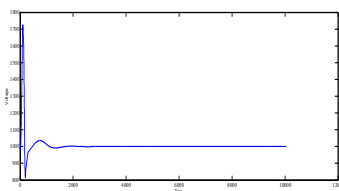
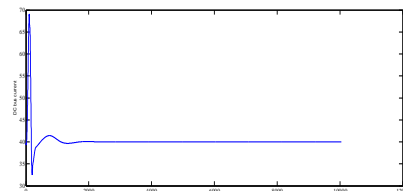


Fig. 5.9 (a) DC Bus Voltage



(b) DC Bus Current

### 5.3.4 Photovoltaic connected to a three-phase inverter

In this simulation, the output of the boost converter is connected to the three-phase inverter and the three-phase resistive load. The simulation model in Fig. 4.5 is used to simulate the three-phase photovoltaic system with  $10 \Omega$  resistive loads on each phase. The carrier frequency is set at 2 kHz and the sampling time is  $2 \times 10^{-6}$  s [23]. The three-phase inverter delivers a three-phase current to the load. Fig. 5.7 shows a sinusoidal load voltage for phase a. The DC voltage produced by the photovoltaic system is converted into AC current to the load for  $V_{ab}$  &  $V_{dc}$ .

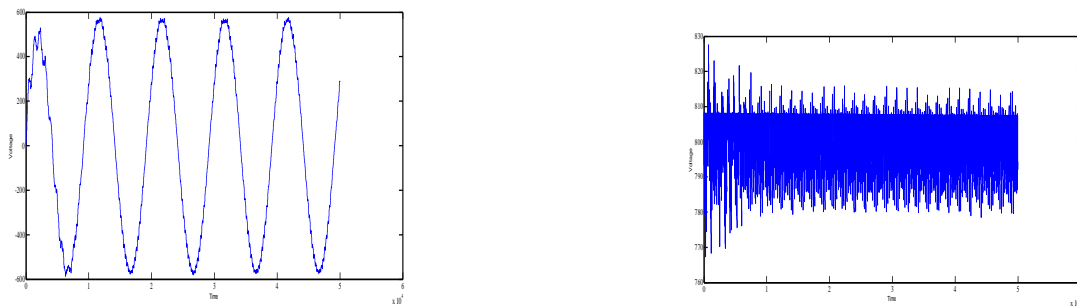


Fig. 5.10 sinusoidal load voltage ( $V_{ab}$  &  $V_{dc}$ )

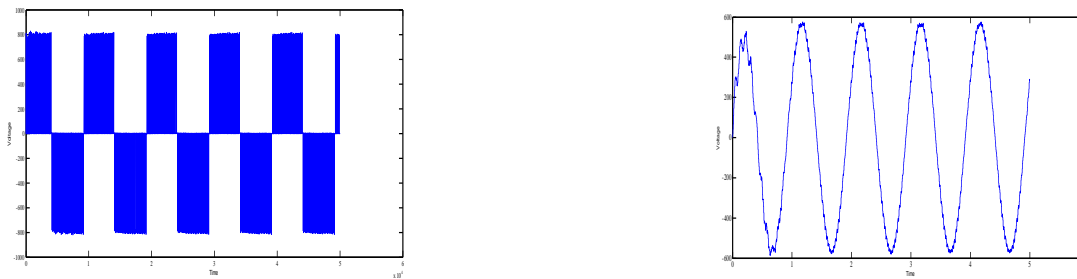


Fig. 5.11 (a)  $V_{ab}$  Inverter (b)  $V_{ab}$  load

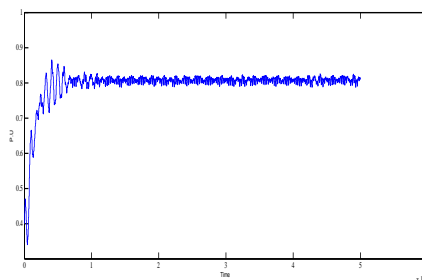


Fig. 5.12 Battery connected to a three-phase inverter (Modulation index)

Fig. 5.11 shows a  $V_{dc}$ ,  $V_{ab}$ , sinusoidal load voltage for  $V_{ab}$  and modulation index. The DC voltage produced by the photovoltaic system is converted into AC current to the load.

Fig. 5.12 is the photovoltaic voltage, inverter voltage, load voltage, modulation index. Without the current control and the voltage control, the DC link voltage is not constant. The voltage of the DC link is dependent of the load. Table 5.6 shows the result of the photovoltaic system connected to the load

TABLE 5.6

PARAMETERS OF 26 KW PHOTOVOLTAIC SYSTEMS

DATA	VALUE	DATA	VALUE
Insolation	1000	$I_{sc}$	43.6
Dc connected current	63.86	$V_{oc}$	888
Dc connected voltage	773.30	$I_{pm}$	39.6
$V_{pv}$	753.7	$V_{pm}$	704
$I_{pv}$	64.49	L	200*e-6 H
$P_{pv}$	26.83kw	C	5000*e-6 F



Fig. 5.13 Vdc Vab Inverter



Fig.5.14 Vab Load Modulation Index

## 5.4 PV system connected with load including MPPT and Battery

### 5.4.1 PV system connected with load including MPPT

In fig 5.13 shows the simulation model of maximum power point controller with PV system. The result of simulation is shown below.

TABLE 5.7

READING OF V, I, P, & D

INSOLATION	RESISTANT	$V_{PV}$	$I_{PV}$	$P_{PV}$	DUTY CYCLE	$V_{OUT}$	$I_{OUT}$
1000	25	105.1	4.85	509.5	0.07679	111.2	4.448
	50	105.1	4.85	509.5	0.3158	150	3.288
	75	105.1	4.85	509.5	0.3158	150	3.288
	100	105.1	4.85	509.5	0.3158	150	3.288
800	25	106.5	3.85	409.9	0.012	95.48	3.82
	50	106.5	3.85	409.5	0.2591	141.1	2.822
	75	106.5	3.85	409.5	0.3029	150	2.654
	100	106.5	3.85	409.5	0.3031	150	2.653

500	25	37.53	2.65	99.45	0.2764	50.03	1.888
	50	37.53	2.65	99.45	0.4717	68.53	1.37
	75	37.53	2.65	99.45	0.5675	83.71	1.116
	100	37.53	2.65	99.45	0.6247	96.46	0.9645

From above table we show that, when we change the value of resistance, there is no effect on voltage, current and power.

#### 5.4.2 PV system connected with load including MPPT and battery

In fig 4.7 shows the simulation model of maximum power point controller and battery with PV system. Table 5.8 shows the value of power and battery charging and discharging process. When insolation is high at that time the battery is charging and at low insolation battery is discharging. Fig shows the waveform of the load

TABLE 5.8

READING OF P & I<sub>BATTERY</sub> (50 KW Load)

INSOLATION	V <sub>PV</sub>	CONVERTER CURRENT
1000	856.4	72.67
800_50_90	849.4	62.97
500_50_90	935.8	29.97
CONVERTER VOLT	CONVERTER POWER	I <sub>PV</sub> MPP
877.1	6.68*10000	78
739	5.351*10000	63
638.5	2.807*10000	30
I <sub>L</sub>	I BATTERY	RMS V <sub>AB</sub>
57.67	15	399.9
72.97	-10	398.9
79.97	-50	390.2



Fig. 5.15 Insolation at 1000 W/m<sup>2</sup> Vdc & V ab Inverter

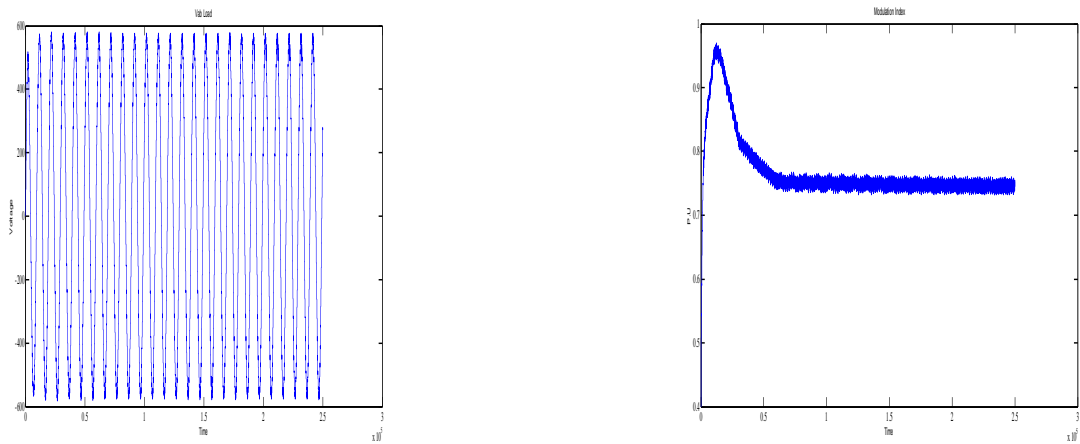


Fig. 5.16 Vab Load & Modulation Index

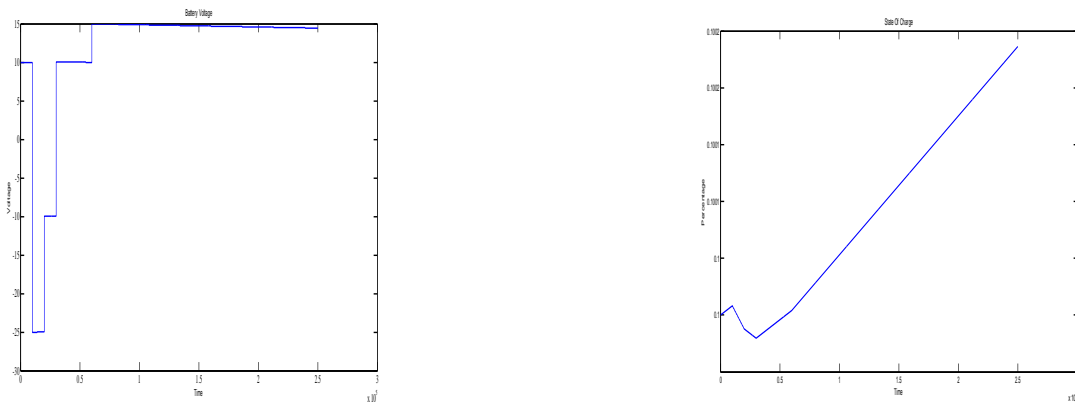


Fig. 5.17 Battery Voltage & State Of Charge

### 5.5 Grid connected PV system

The simulation model of grid connected PV system. The result of simulation is shown below.

TABLE 5.9

READING OF GRID CONNECTED SYSTEM AT DIFFERENT INSOLATION

INSOLATION	$V_{PV}$	CONVERTER CURRENT	CONVERTER VOLT	CONVERTER POWER	$I_{PV}$ MPP	$V_{dc}$
1000	856.4	66.72	955.3	6.68*10000	78	955.3
800	849.4	58.48	881	5.351*10000	63	881
500	846.8	38.57	618.1	3.269*10000	38.6	618.3

Now the waveform shows the voltage, current, active and reactive power, terminal voltage and  $V_{abc}$  at input side and infinity bus,  $I_{abc}$  at infinite bus.

**Insolation at 1000 W/m<sup>2</sup>**

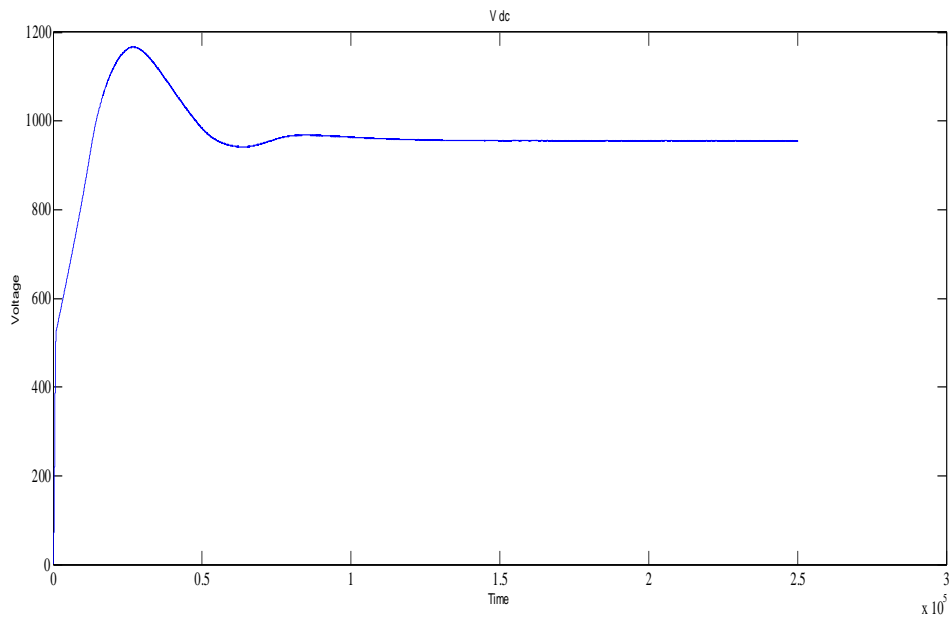


Fig. 5.18 Vdc



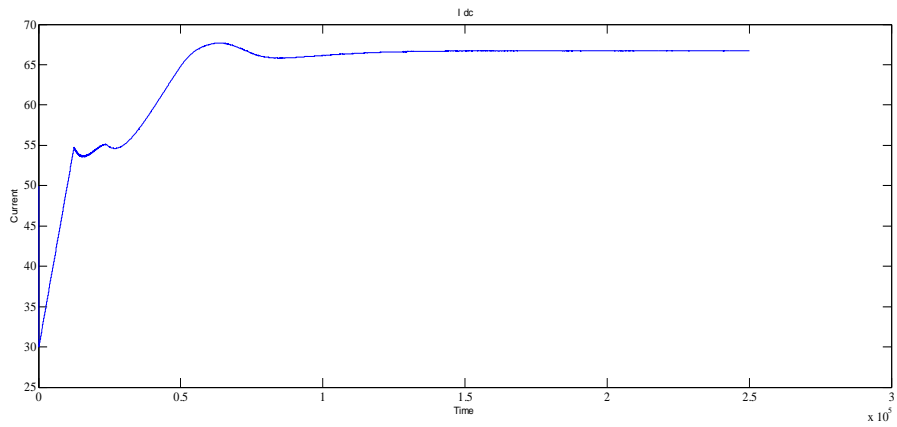
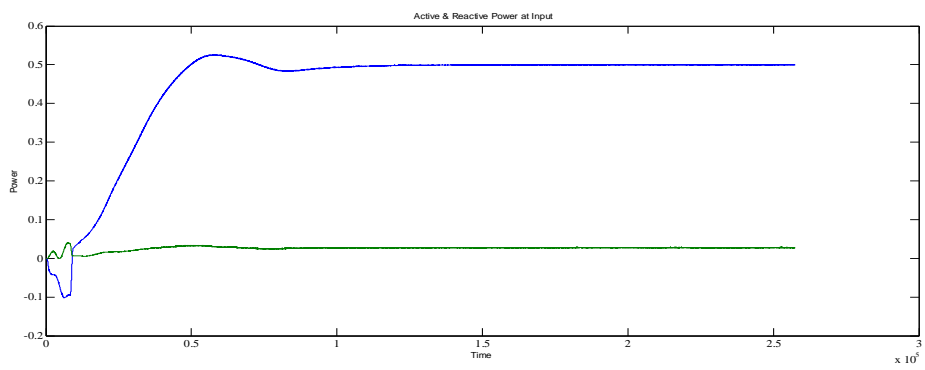


Fig. 5.19 waveform of DC bus I dc

Active & Reactive power (I/P)



Active & Reactive power (I/B)

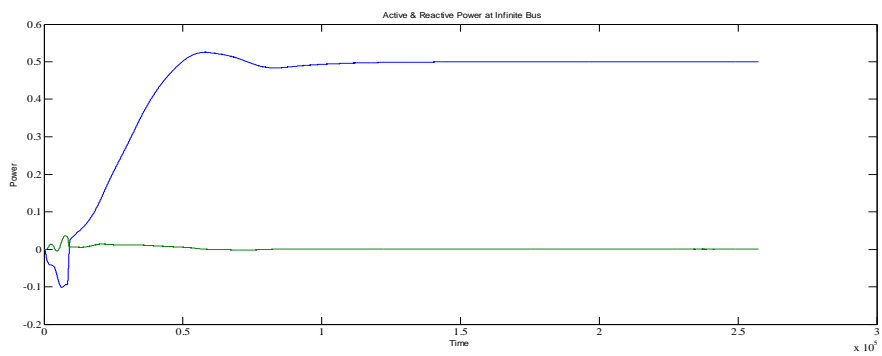
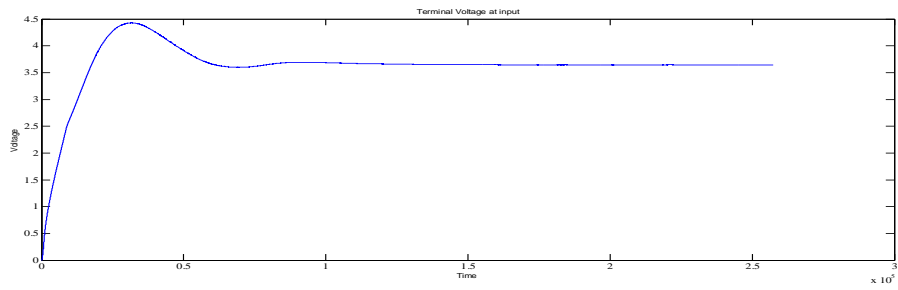


Fig. 5.20: waveform of active and reactive power

### Terminal Voltage (I/P)



### Terminal Voltage (I/B)

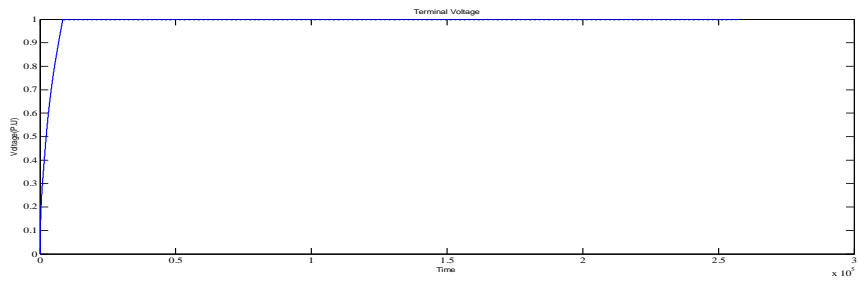
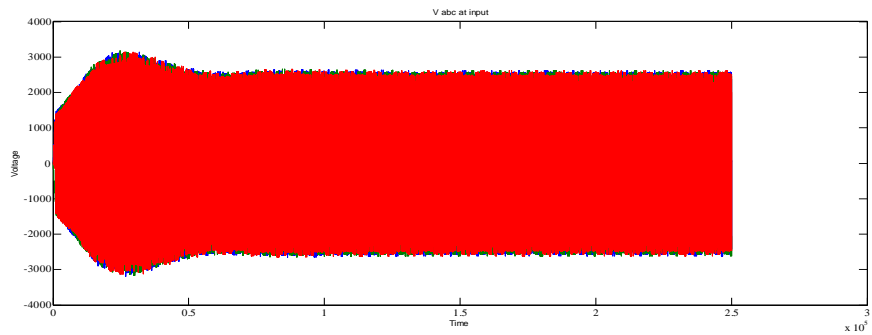
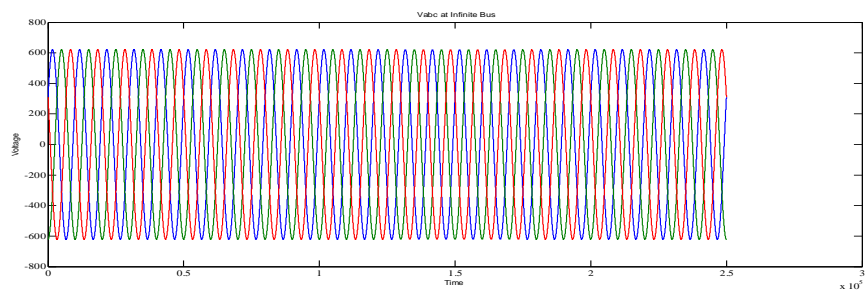


Fig. 5.21: waveform of terminal voltage

### Vabc (I/P)



### Vabc (I/B)



Iabc (I/B)

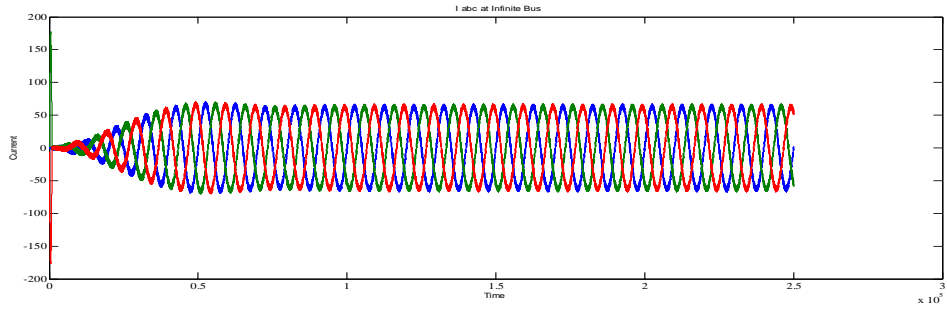


Fig. 5.22: waveform of  $V_{abc}$  and  $I_{abc}$

Insolation at  $800 \text{ W/m}^2$

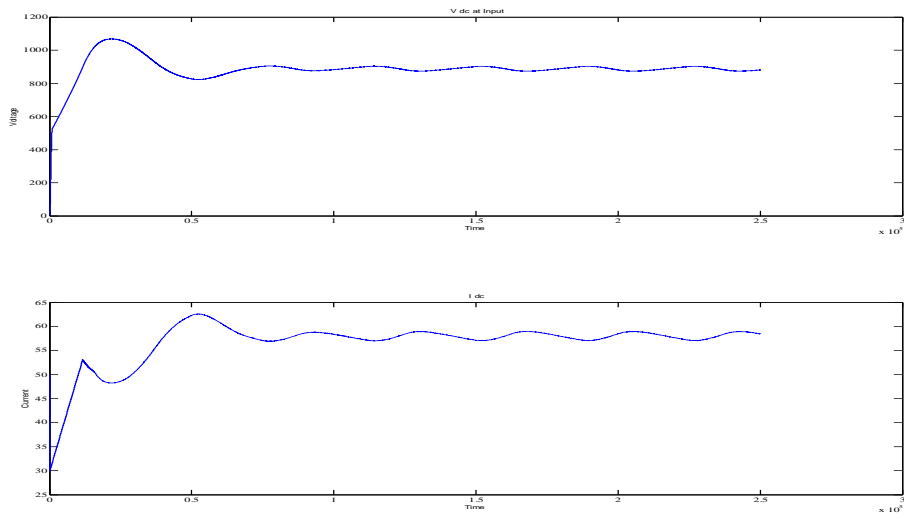


Fig. 5.23: waveform of DC bus  $V_{dc}$  &  $I_{dc}$

Active & Reactive power (I/P) Active & Reactive power (I/B)

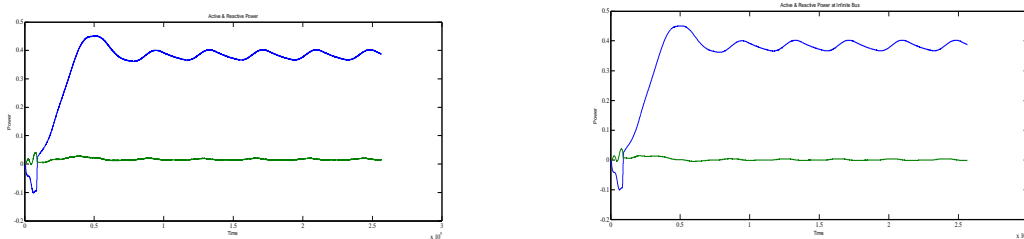
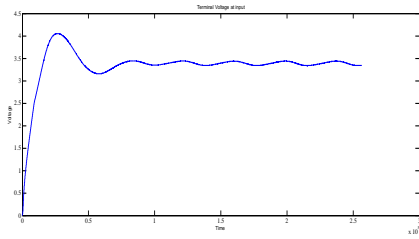


Fig. 5.24: waveform of active and reactive power

Terminal Voltage (I/P)



Terminal Voltage (I/B)

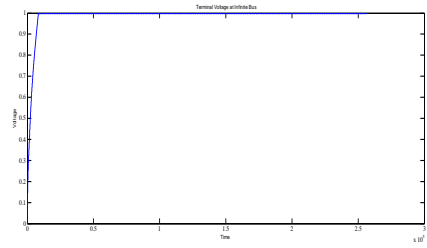
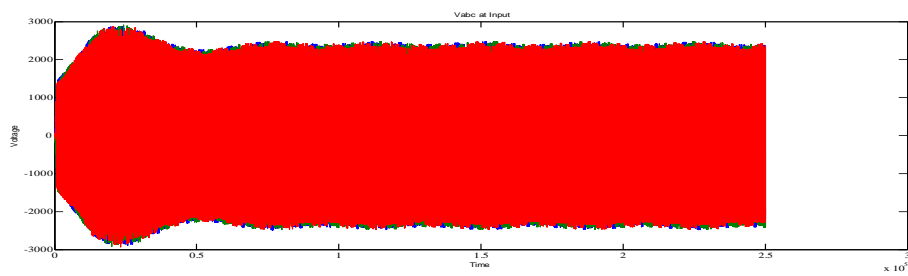
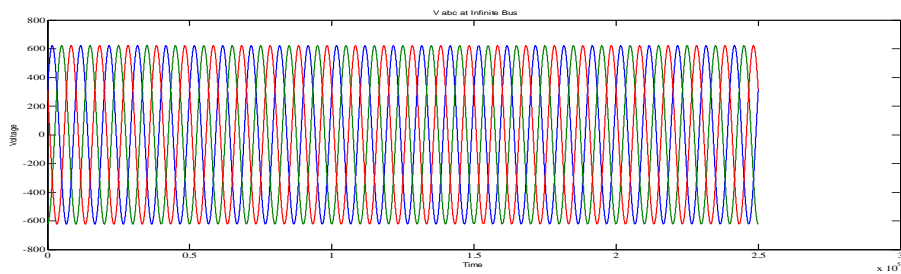


Fig. 5.25: waveform of terminal voltage

Vabc (I/P)



Vabc (I/B)



Iabc (I/B)

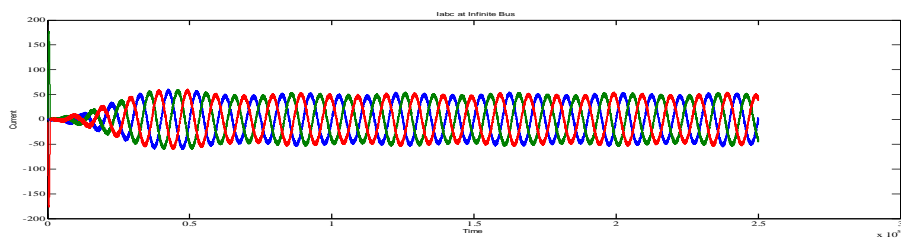
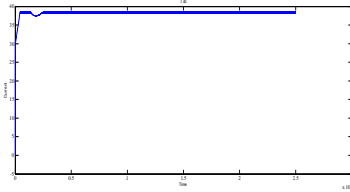


Fig. 5.26: waveform of  $V_{abc}$  and  $I_{abc}$

## Insolation at 500 W/m<sup>2</sup>

I<sub>dc</sub>



V<sub>dc</sub>

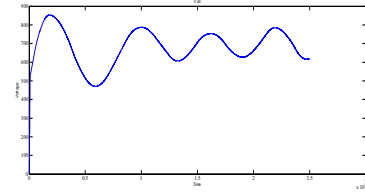
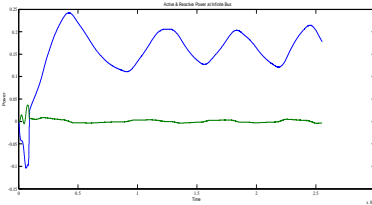


Fig. 5.27: waveform of DC bus

Active & Reactive power (I/B)



Active & Reactive power (I/P)

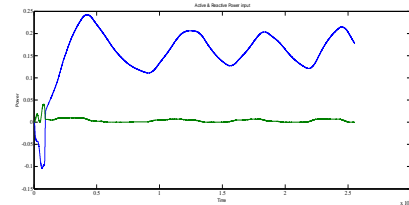


Fig. 5.28: waveform of active and reactive power

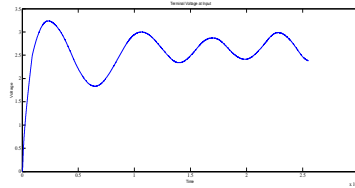
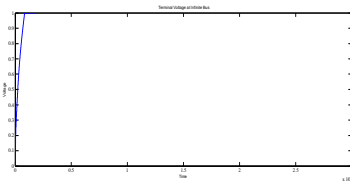
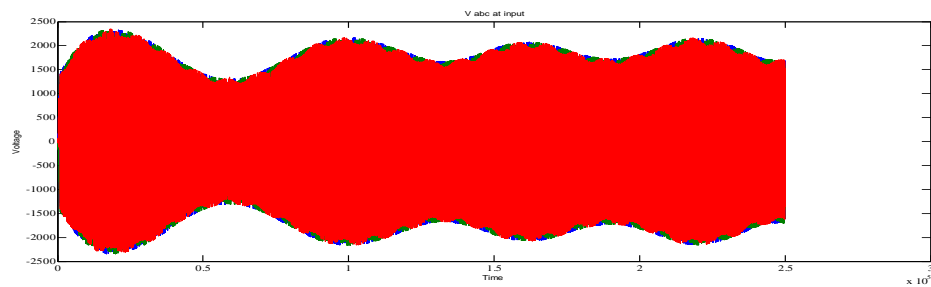


Fig. 5.29: waveform of terminal voltage



Vabc (I/B)

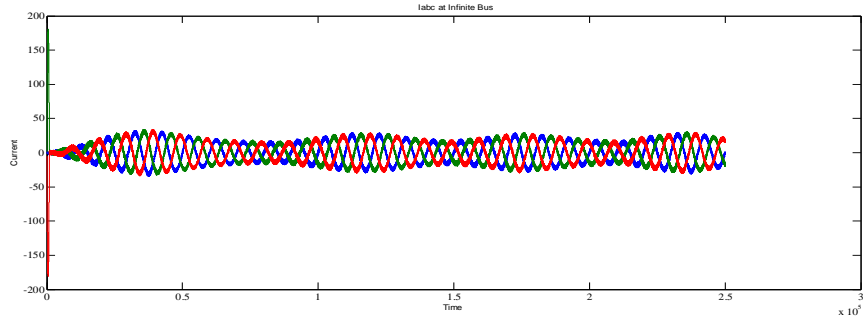
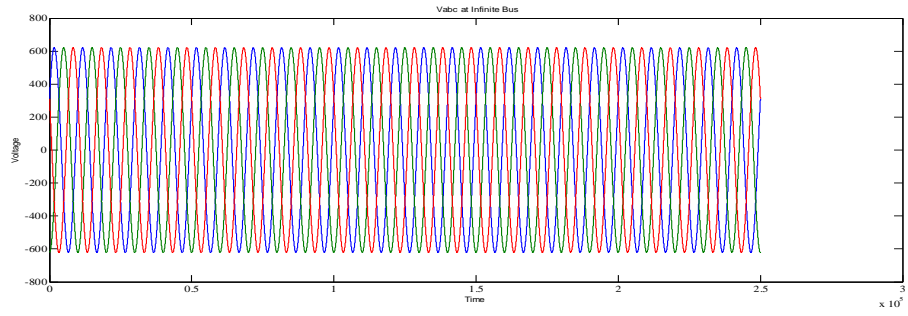


Fig. 5.30 waveform of  $V_{abc}$  and  $I_{abc}$

## **CHAPTER 6**

### **CONCLUSION**

#### **6.1 Conclusion**

In this thesis, the study of the photovoltaic system with maximum power point controller has been developed. From the theory of the photovoltaic, a mathematic model of the PV has been presented. Then, the photovoltaic system with DC-DC boost converter; maximum power point controller and resistive load have been designed. Finally, the system has been simulated with Simulink /MATLAB.

First, the simulations of the PV panels showed that the simulated models were accurate to determine the characteristics voltage current because the current voltage characteristics are the same as the characteristics given from the data sheet. In addition, when the irradiance or temperature varies, the PV models output voltage current change. Then, the simulation showed that Perturb and observe algorithm can track the maximum power point of the PV, it always runs at maximum power no matter what the operation condition is. The results showed that the Perturb and observe algorithm delivered an efficiency close to 100% in steady state.

The simulations of the PV with maximum power point, boost converter and resistive load were performed by varying the load, the irradiance.

Finally, the PV performance and the maximum power point was analyzed, and the three phase full bridge DC-AC inverter was simulated with grid. The results showed that the DC voltage generated by the PV array could produce an AC current sinusoidal at the output of the inverter. The amplitude of the current depends on the PV power.

#### **6.2 Future scope**

The proposed topology may be further implemented with Hybrid system. A fully digitized implementation of the proposed system can be carried out through the development of programmable tie-line control of Hybrid system. We can develop a master grid to excess of energy, connected with the different sources.

## REFERENCES

### PAPERS

- [1] A Photovoltaic Array Simulation Model for Matlab-Simulink GUI Environment, by Yun Tiam Tan, Student Member, IEEE, Daniel S. Kirschen, Senior Member, IEEE, and Nicholas Jenkins, Senior Member, IEEE.
- [2] M.G.Villalva, J.R. Gazoli, E. Ruppert F. Modelling and Circuit Based Simulation of Photovoltaic Arrays University of Campinas-Brazil.
- [3] Huan-Liang Tsai “Development of Generalized Photovoltaic Model using Matlab/Simulink, 2008.
- [4] I.H. Altas “A Photovoltaic Array Simulation Model for Matlab-Simulink GUI Environment” Dept of Electrical and Electronics Engineering, Karadeniz Technical University, Trabzon, Turkey.
- [5] Hasaneen, B.M. and Elbaset Mohammed, A.A., “Design and simulation of DC/DC converter,” *Power System Conference, 2008. MEPCON 2008. 12th International Middle-East*, July 2008, pp. 335 - 340.
- [6] Weiping Luo and Gujing Han, “Tracking and controlling of maximum power point application in grid-connected photovoltaic generation system,” *Second International Symposium on Knowledge Acquisition and Modeling 2009, KAM '09*, vol. 3, December 2009, pp. 237 - 240.
- [7] Antunes, F.L.M., Santos, J.L., “Maximum Power Point Tracker for PV Systems,” World Climate & Energy Event, December 2003.
- [8] R.Faranada, S.Leva and V.Maugeri MPPT techniques for PV System; energetic & cost comparison, Member IEEE.
- [9] Grid-connected photovoltaic (PV) systems with batteries storage as solution to electrical grid outages in Burkina Faso D Abdoulaye, Z Koalaga, F Zougmore, 1st



International Symposium on Electrical Arc and Thermal Plasmas in Africa (ISAPA), IOP Conf. Series: Materials Science and Engineering 29 (2012) 012015.

- [10] Zhou Dejie, Zhao Zhengming, Eltawil, M. and Yuan Liqiang; "Design and control of a Three-phase Grid connected Photovoltaic system with developed Maximum power point tracking," *Applied Power Electronics Conference and Exposition, 2008. APEC 2008. Twenty-Third Annual IEEE*, May 2008, pp. 973 - 979.
- [11] Liang Ma, Wang Ran and Zheng, T.Q., "Modeling and Control of 100 kW Three-phase grid-connected Photovoltaic inverter," *Industrial Electronics and Applications (ICIEA), 2010 the 5th IEEE Conference*, July 2010, pp. 825 - 830.

## APPENDIX

### Appendix - A

TABLE A -1

#### S.I.UNIT

S.N.	Physical Quantity	Unit	Abbreviation
1	Length	Meter	M
2	Mass	Kilogram	Kg
3	Time	Second	S
4	Temperature	Kelvin	K
5	Electrical Current	Ampere	A
6	Amount	Mole	Mole

### Appendix - B

TABLE A -2

#### Derived S.I. UNIT

S.N.	Physical Quantity	Unit	Abbreviation
1	Force	Newton	N
2	Pressure	Newton/Square meter	N/Sq. m
3	Work	Joule	J
4	Heat	Joule	J
5	Power	Watt	W
6	Torque	Newton meter	N-m
7	Dynamic velocity	Newton second/Square meter	N- sec/Sq.m
8	Kinematic viscosity	Stoke	Cm <sup>2</sup> /s
9	Specific heat	Joule per Kg per degree Kelvin	J/Kg K
10	Thermal conductivity	Watt per meter per degree Kelvin	W/m K

**BABU BANARASI DAS UNIVERSITY**

**Plagiarism Report**

**Student Name: Mr. Vivek Kumar Singh**

**Roll No.: 1170450006**

**Thesis Title: END USER VOLTAGE REGULATION AT LOW-VOLTAGE  
DISTRIBUTION CONGESTION OF BATTERY CONNECTED MICRO-GRID**

**Guide:**

**VIKASH PANDEY**

**Assistant Professor**

Department of Electrical Engineering

School of Engineering

Babu Banarasi Das University, Lucknow.

**Plagiarism report details**

**87.8% (Unique contents)**

**12.2% (Plagiarism)**

## **LIST OF PUBLICATION**

### **PAPER-I**

- ❖ **DESIGN OF SMALL POWER STAND ALONE SOLAR PHOTOVOLTAIC ENERGY SYSTEM**

IJERCSE Vol6, Issue 4, April 2019 ISSN Number 2394-2320

Impact factor: 4.890

Vivek Kumar Singh<sup>1</sup>, V.K. Maurya<sup>2</sup>, Vikas Pandey<sup>2</sup>

1: M.Tech scholar Department of Electrical Engineering

2: Assistant Professor Department of Electrical Engineering

Babu Banarasi Das University Lucknow, Uttar Pradesh, India

### **PAPER-II**

- ❖ **SIMULATION RESULT ON VOLTAGE REGULATION OF SMALL POWER STAND ALONE SOLAR PHOTOVOLTAIC ENERGY SYSTEM**

IJAERD Vol6, Issue 4, April 2019 e-ISSN Number 2348-4470

Impact factor: 5.71

Vivek Kumar Singh<sup>1</sup>, V.K. Maurya<sup>2</sup>, Vikas Pandey<sup>2</sup>

1: M.Tech scholar Department of Electrical Engineering

2: Assistant Professor Department of Electrical Engineering

Babu Banarasi Das University Lucknow, Uttar Pradesh, India

**BABU BANARASI DAS UNIVERSITY, LUCKNOW**  
**CERTIFICATE OF FINAL THESIS SUBMISSION**

**1. Name: Vivek Kumar Singh**

**2. Roll No: 1170450006**

**3. Thesis title: END USER VOLTAGE REGULATION AT LOW-VOLTAGE DISTRIBUTION CONGESTION OF BATTERY CONNECTED MICRO-GRID**

4. Degree for which the thesis is submitted: **Master of Technology (Power System & Control)**

5. School (of the university to which the thesis is submitted)

**School of Engineering**

6. Thesis Preparation Guide was referred to preparing the thesis.	YES	NO
7. Specifications regarding thesis format have been closely followed.	YES	NO
8. The content of the thesis have been reconized based on the Guidelines.	YES	NO
9. The thesis has been prepared without resorting to plagiarism.	YES	NO
10. All source used have been cited appropriately.	YES	NO
11. The thesis has not been submitted elsewhere for a degree.	YES	NO
12. All the correction have been incorporated.	YES	NO
13. Submitted 4 hard bound copies plus one CD.	YES	NO

(Signature of Guide)

(Signature of Candidate)

## CURRICULUM VITAE

**VIVEK KUMAR SINGH**

**Mobile:** +91-8052986339

**E-mail:** rajputvivekrv898630@gmail.com



### CAREER OBJECTIVE

To become a successful professional and a strong asset for any growing industry through innovative ideas, dedication, enthusiasm and team spirit.

### EDUCATIONAL QUALIFICATION

Degree/Course	College/School	University/ Board	Year of Passing	% Marks
B.Tech (Electrical Engineering)	B. N. College of Engineering and Technology, Lucknow	Dr.A.P.J.Abdul Kalam Technical University, Lucknow	2017	73.28%
Intermediate	S S M V M V GRAM BHARTI PARTOSH CP S NGR	Uttar Pradesh Board Allahabad	2012	61%
High School	S S M VM V GRAM BHARTI DHAMMAUR SULTANPUR	Uttar Pradesh Board Allahabad	2010	61%

### TECHNICAL SKILLS

- Proficient knowledge of MS Office.
- Languages known: C, C++

### PROJECTS

#### • MEGA PROJECT

- Title : **MICROCONTROLLER BASED FOUR QUADRANT SPEED CONTROL OF BLDC MOTOR**
- Team Size : 4
- Description : Controlling the speed of DC Motor

### INDUSTRIAL TRAININGS/WORKSHOPS

- Organization : HINDALCO INDUSTRIES LIMITED  
(Renusagar Power Division)  
Sonebhadra
- Duration : 3 Weeks
- Description : Motor & Transformer Protection